学位論文

LIFE EXPECTANCY OF JOMON PEOPLE ESTIMATED FROM THE DENTAL PULP VOLUMES BY BAYESIAN APPROACH

（歯髄腔容積を用いてベイズ法により推定した縄文時代人の平均余命）

平成２５年１２月博士（理学）申請

東京大学大学院理学系研究科
生物科学専攻

佐々木　智彦

Abstract

The Jomon period is one of Japanese prehistoric periods which began about 13,000 years BP and lasted roughly 10,000 years thereafter. Human life span (longevity) during the Jomon period is interesting when compared with those of the succeeding periods, which enables to shed light on the substantial change in ecology, subsistence and society over the human population history of Japan. In broader perspectives, it is also interesting as it provides an insight into the evolution of human life history which distinguishes humans from the other primates. The longevity of Jomon people has been previously estimated from the skeletons by Kobayashi (1967) where it was represented by the life expectancy at age 15. The result was 16.1 years for males and 16.3 years for females. However, the age estimation method he employed included a statistical problem. Assignment of age to the skeleton referring to known ages of skeletons with similar aging expression is classified as inverse regression in statistical terms. It has been pointed out that the age estimation by inverse regression is to be influenced by the age distribution of the reference sample, and the reconstructed age distribution is to mimic that of the reference sample (Bocquet-Appel and Masset, 1982). Since the reference sample used by Kobayashi (1967) was composed dominantly of young adult individuals, a number of Jomon ages should have been underestimated in his study.

To circumvent the problem, I adopted Bayesian approaches. Bayesian approaches use reference sample to derive the probability to obtain an expression of the age indicator for an individual of certain age. This is classified as forward regression, and not influenced by the age distribution of the reference sample.

Furthermore, another problem might have distorted the estimation by Kobayashi (1967). Different durability of bones against taphonomic processes presumably filters out the fragile old skeletons. This could make the estimation of ancient mortality distribution younger than the reality because the skeletons observed by researchers would under-represent the deaths of the old individuals. While bones are likely differentially preserved because the remodeling activity declines throughout the life, teeth are less likely on this regard because remodeling does not occur in teeth. To minimize the effect of differential preservation, I used teeth as the age indicator for Jomon skeletons.

The pulp cavity in teeth reduces with age due to dentin apposition on the pulp wall through the life. I utilized the pulp volume ratio (PVRrt: volume proportion of the pulp cavity in the root portion) as the age indicator. Those volumes were measured on the digital imageries obtained by microfocus computed tomography (micro-CT). I scanned 363 recent-modern Japanese lower canines and established a statistical model to describe the probability distribution of the PVRrt according to age.

Next, the PVRrt values were observed on lower-canines from 234 Jomon individuals stored in The University Museum, The University of Tokyo (UMUT). As in Kobayashi (1967), the observations were limited to those individuals considered at or above age 15. Sexes were not separated in this study to avoid too much statistical assumptions in the Bayesian approaches.

Bayesian approaches update the probability (called prior probability) of the subject to new one (called posterior probability) by applying the information from observations. The information (called likelihood) is the probability to obtain the observations when a certain hypothesis about the subject is assumed. In this dissertation, 5 parameters (α, β, γ, λ, θ) specify the hypothesis, among which α and β specify the

age-at-death distribution of Jomon people. The prior probability of those parameters (collectively denoted as Ω) can be updated by the likelihood to the posterior probability using Bayes' theorem,

$$p(\Omega \mid z_1,....,z_{234}) = \frac{g(\Omega)\cdot L(\Omega)}{\int_\Omega g(\Omega)\cdot L(\Omega)\cdot d\Omega},$$

where $z_1,....,z_{234}$ are the observations on 234 Jomon individuals, $g(\Omega)$ is the prior probability function, and $L(\Omega)$ is the likelihood function on the observations $z_1,....,z_{234}$. Here, I explain what those 5 parameters stand for, while explaining the components of the likelihood function. The start point for the likelihood calculation is to formulate the probability (density) for an individual i to be at age x *and* have an age-expression z_i. This probability was computed by multiplications of the following four probabilities:

(1). $p(x \mid \alpha, \beta)$: the probability density for a Jomon individual (with lower canine) to be at age x. This was formulated by a modified demographic model which was specified by α and β.

(2). $p(\mathrm{PVRrt} \mid x, \gamma)$: the probability density of PVRrt value at age x, parameterized with a statistical model derived from the recent-modern Japanese samples. γ is the parameter which specifies the rate of PVRrt reduction. It was set as one of the target to give the posterior probability distribution by Bayesian approaches to consider the possibility that the rate of reduction could be different in Jomon people from that of recent-modern Japanese .

(3). $p(\mathrm{epiphyseal\,state} \mid x)$: the age-conditional probability of the state of epiphyseal closure at sternal end of the clavicle. It was either "complete" or "incomplete." This additional age information was necessary to compensate for the unknown PVRrt reduction rate γ for Jomon people. This probability was set as 1 when clavicles were not preserved for the individual.

(4). $p(\mathrm{clavicle\,preservation} \mid x, \lambda, \theta)$: the age-conditional probability for an individual with the lower canine to preserve the clavicle for the epiphyseal observation. The parameters λ and θ describe the change in the probability with age, and the posterior probability distributions were given to them by Bayesian approaches.

The observation z_i denotes the set of (2)–(4) observations. Integrating the multiplication of the four probabilities for whole age range gives the probability to have the observation z_i for the individual i. The likelihood function was composed of multiplication of this probability for the 234 Jomon individuals.

Before conducting Bayesian approach, the maximum likelihood estimation was calculated for the life expectancy of Jomon people at age 15 (e_{15}), to compare the estimation with that by Kobayashi (1967). The maximum likelihood is the method to seek the parameter set which maximizes the likelihood function. The life expectancy at 15 calculated from the maximum likelihood estimate was 30.6 years. To test the difference of this result from that of Kobayashi (1967), pseudo-estimations of e_{15} were calculated from 234 pseudo-samples generated computationally upon the null hypothesis that the age-at-death distribution in Kobayashi (1967) was true. While the set of pseudo-samples were generated 500 times, the estimation from the real Jomon samples was larger than all the pseudo-estimations, indicating that the Jomon population from which the samples used in this study were extracted is significantly older than the age-at-death distribution estimated by Kobayashi (1967).

The prior probability is that for the five parameters (α, β, γ, λ, θ) *before* obtaining the observations. I suppose that the ideal prior is the distribution of those parameters hypothetically to be achieved by a number of human populations with similar genetic compositions and similar living environments to those of Jomon people. Since such information is not available, I used uniform prior distributions. However, some prior information about the parameters for age-at-death distribution (α, β) could be obtained from modern and historical human life tables. A scatter diagram of the life expectancy at age 15 (e_{15}) and the coefficient of variation of the years-to-death after age 15 (CV) indicated a human specific tendency for their survival profiles, which was distinct from that of other primates. This tendency enabled a non-uniform prior probability distribution for α and β. From the human distribution on the diagram, the non-uniform prior for α and β was calculated. This prior should be closer to the ideal one than is the uniform prior.

The posterior probability distribution was calculated from the above-mentioned prior probability distributions and the likelihood function. When uniform priors were used for all the parameters, the 95% credible interval (defined as the interval between 2.5 percentile and 97.5 percentile values of the posterior probability distribution) of the life expectancy at age 15 was 19.5–43.6 years. The mean value was 29.5 years. When the non-uniform prior was applied to α and β and uniform priors to the rest, the 95% credible interval was 29.2–41.5 years. The mean was 35.2 years.

As the conclusion, the life expectancy for Jomon people at age 15 was substantially older than that estimated by Kobayashi (1967). The possible range is 19–44 years. With the human pattern of survival profile considered, I suppose that 29–42 years is the most probable range of the expected years for Jomon people at age 15.

Acknowledgements

Since I started to study anthropology in 2009, I have been encouraged by a lot of people. First and foremost, I owe this work and things I have learned in this university to Dr. Osamu Kondo. When I joined in his laboratory as a graduate student, I did not have a definite aim in my research (and for my career). My interest frequently changed. But thanks to him, I could follow my interest anytime. No matter how I changed my direction, he supported my will and helped me as much as he could.

I also thank Dr. Gen Suwa for a lot of help and invaluable advice and for giving me credit for operating CT machines and using the skeletal samples in his laboratory. And I thank Drs. Eisaku Kanazawa, Yasuhisa Tsujimoto, Mitsuko Nakayama, and Yoko Wada for accommodating my request for the teeth samples used in this study. A special thank must be given to the members of Kondo lab. and Suwa lab. for their kind support and a lot of advice.

Last but not least, I thank my parents for respecting my choice and wishing my success anytime.

Contents

List of tables

List of figures

Chapter I

Jomon people and previous studies about their longevity

This chapter reviews the archaeological and anthropological knowledge about the Jomon people, and introduces the pioneering study by Kobayashi (1967) for their life span (longevity). There, I will argue a statistical problem in the method he employed to estimate the ages of the Jomon skeletons, and discuss the methods to circumvent the problem.

The Jomon period

Jomon pottery—meaning “cord marked pottery”—is a type of pottery which can be popularly identified in many Japanese archaeological sites. The Jomon period characterized by the pottery is one of Japanese prehistoric periods, succeeding the Paleolithic and followed by the Yayoi period. Beginning of the period dates back to Pleistocene–Holocene transition ca. 13,000 years BP (Nakamura et al., 2001), and the end is marked by a propagation of wet rice agriculture to the Japanese archipelago from the Asian continent ca. 3,250–2,100 years BP (Keally and Muto, 1982).

People during the Jomon period are believed to have been hunter-gatherers with sedentary lifestyles. While indications of horticulture and arboriculture are accumulating through an amount of recent research, contribution of those activities to their lifestyles has been thought to be small compared to hunting and gathering for abundant wild food resources (Matsui and Kanehara, 2006). Archaeological remains indicates that their food resources included deer, wild boar, tuna, bream, salmon, whale, sea lion, clams, chestnuts, acorns, yam, etc., although the availability and exploitation of them seem to have varied depending on the locations in Japanese archipelago (Akazawa, 1986; Minagawa and Akazawa, 1992; Kusaka, et al., 2010; Naito, et al., 2013). Their settled lifestyles to some extent are evident in remains of the pit-dwellings. However, the degree of the sedentism (whether full or temporary settlement) have yet to be revealed (Habu, 2004).

Genetic contribution from Paleolithic inhabitants in Japanese archipelago to Jomon populations is unknown. As to that from Jomon to modern Japanese, Hanihara (1991) hypothesized that the fundamental gene pool of the modern Japanese population had been composed of a mixture of two lineages: Jomon and populations migrated from northeast Asia at the end of Jomon and the following aeneolithic-protohistoric period. Supporting his hypothesis, the genetic contribution of Jomon population to modern Japanese was confirmed recently by ancient mitochondrial DNA analysis (Adachi, et al., 2009).

As for funeral practices, Jomon people commonly buried the dead. Both primary and secondary burials existed. The most common style was the primary burial with a simple pit without cremation (Habu, 2004). For fetus or newborn, a burial into a jar seemed common (Kikuchi, 1983). Some variations of secondary burials including “collective” burials (mixture of multiple bodies) and “square-shaped bone-pile” burials (long bones are arranged to shape squares), and cremations have been occasionally identified (Habu, 2004).

Life expectancy estimation by Kobayashi (1967)

Since the end of 19th century, a number of Jomon skeletal specimens had been excavated from archaeological sites in Japan, which allowed Kazumasa Kobayashi to estimate the life history of Jomon people on the basis of those skeletons with several age estimation techniques. In 1964, he preliminary investigated 38 Jomon skeletons, in which he estimated their ages primarily based on metamorphosis of the pubic symphysis. In his paper in 1967, he expanded the study to include 235 Jomon individuals examining a variety of age indicators, i.e., besides the pubic metamorphosis, those of auricular surface of ilium, epiphyseal fusion and the osteophytosis or “lipping” in various skeletal parts, etc. Corresponding ages to those indications were derived from modern Japanese skeletons of known age and sex. He limited the age assessment to the skeletons assumed to be at or above 15 years of age due to lack of infants and children in the collection. He wrote

> “(i)n the course of examining skeletal remains for age estimation, it was noticed by the author that skeletons of infants and children in the collection were too scanty in general through all the (Japanese) periods to reveal any appropriate level of pre-adult mortality.”

As many life tables of world-wide human populations indicate, the mortality of the first few years of life is relatively high, and this tendency is more remarkable in pre-industrial society. The scantiness of infant and child skeletons in the Jomon collection might have been due to reasons that immature skeletons are so fragile that they seldom survive taphonomic processes, except the case where they had been stored in a jar as mentioned above. In the end, Kobayashi estimated the age-at-death distribution for Jomon people who had reached 15 years of age or older. By averaging the age-at-deaths and subtracting 15 years from it, he estimated the life expectancies at age 15 (given the assumption of stationary population) to be 16.1 years for males and 16.3 years for females.

However, the age estimation method he adopted is problematic in its statistical manner. Assignment of an age to the expression of age indicator was accomplished by referring to the ages of skeletons with the similar expression. This is classified as an inverse regression (or inverse calibration) in statistical terms. Bocquet-Appel and Masset (1982) pointed out that the estimated age by the inverse regression is to be influenced by the age distribution of the reference skeletons. When X is an independent variable and Y is a dependent variable which is determined depending on X with a certain distribution of error, the regression analysis of X on Y in order to estimate new X (x0) from new Y (y0) is called inverse regression. In the case of age estimation, age should be X and age indicator be Y, as it is more natural to assume that the expression of age indicator is determined depending on how long the person has lived (i.e., age) with a certain random variation (caused by such as nutritional variations, etc.), than to assume the reverse. In other words, it may be stated that age and age indicators are in a causal relationship such that age is (one of) the cause and age indicator(s) is the consequence(s) but not vice versa. Figure 1 illustrates an example that the result of inverse regression is to be influenced by the distribution of independent variable X. When the age distribution of reference samples is younger than that of target samples, the inverse regression underestimates the ages of the target samples, and in the opposite case, the inverse regression overestimates the ages of them. As a result, an age distribution reconstructed by such estimations is to be distorted toward the age distribution of the reference skeletons. Figure 2 shows the age distribution of the reference skeletons that Kobayashi used in his study of 1967. As the younger skeletons were dominant in the reference, a

number of Jomon ages should have been underestimated in his study, unless the real age distribution of the Jomon skeletons was coincidentally the same as or even younger than that of the reference skeletons.

Methods to circumvent the influence of the reference-sample's age distribution

Summating Bayesian approaches

Many researchers suggest Bayesian approaches to circumvent the influence of age distribution of reference samples. Bayesian approaches use the probability distribution of age indicators on an individual of certain age. Deriving this probability from the data of reference sample is classified as a forward (or normal) regression. Contrary to the inverse regression, the result of forward regression is not influenced by the distribution of independent variable(s) (Figure 1). If one use the Bayesian theorem to estimate the age of *an* individual, the probability of being at age x when the individual has an age indicator y is calculated as

$$\Pr(x \mid y) = \frac{\Pr(x) \cdot \Pr(y \mid x)}{\sum_{all\ x} \Pr(x) \cdot \Pr(y \mid x)}, \tag{1.1}$$

where $\Pr(x)$ is the probability of being x and $\Pr(y \mid x)$ is the probability of being y conditional on being x. However, in the case of paleodemography, $\Pr(x)$ is unknown (in fact, this is the one we are aiming to estimate). Nagaoka et al. (2007) used a uniform distribution for $\Pr(x)$. Based on the metamorphosis of iliac auricular surface, they calculated the probability distribution of age for each of 86 Jomon individuals using the equation (1.1), and constructed the age-at-death distribution by summating those individual age probabilities. The life expectancy at age 15 was 31.5 years. This method sure is independent from the age distribution of reference samples; however, assuming the uniform distribution has no biological reasoning. The similar approach has been adopted by another researcher for another unearthed skeletal collection. Storey (2007) estimated the age-at-death distribution of skeletons from Mayan archaeological site, Copan, Honduras. She used a model human age distribution (the West 1 model, Coale and Demeny, 1966) for $\Pr(x)$, and summated the individual age probabilities to obtain the age-at-death distribution. As a matter of fact, however, using a model distribution is not a fundamental solution to the

problem. The problem is not what kind of $\Pr(x)$ should be used, but in the presupposition of $\Pr(x)$ itself. The above mentioned approaches—which in this dissertation I refer to *summating Bayesian*—apply the Bayesian theorem inappropriately. Bayesian theorem is used to update the probabilities assigned to some each-competing hypotheses by applying new information obtained by the observations. In this frame of methodology, "probabilities assigned to hypotheses of age-at-death distribution" is the subject to be updated, "probabilities assigned to hypotheses of an individual's age" is not yet. The latter can be the subject *only after* the age-at-death distribution is properly estimated (Hoppa and Vaupel, 2002). In addition, it is one of the merits of a Bayesian approach that we can obtain the resultant probability distribution as a measurement of plausibility of the competing hypotheses. The summating Bayesian can not produce such a measurement to assess the plausibility of the estimation.

Non-model-based and model-based Bayesian approaches

As described in Di Bacco et al. (1999), the Bayesian theorem which applies to the estimation of age-at-death distribution is written as

$$\Pr(F_t \mid y_1,....,y_n) = \frac{\Pr(F_t)\cdot \Pr(y_1,....,y_n \mid F_t)}{\sum_{all\, F_t \in F} \Pr(F_t)\cdot \Pr(y_1,....,y_n \mid F_t)}, \tag{1.2}$$

where F_t denotes an age-at-death distribution, $y_1,....,y_n$ denotes the set of age indicator expressions observed on n skeletons, and F is the set of all possible F_t. $\Pr(F_t)$—which is called a *prior probability* in terms of Bayesian inference—is the probability assigned to F_t *before* obtaining the observations $y_1,....,y_n$. $\Pr(y_1,....,y_n \mid F_t)$—which is called a *likelihood*[*]—is the probability that $y_1,....,y_n$ will be observed when the age-at-death distribution is assumed to be F_t. $\Pr(F_t \mid y_1,....,y_n)$ is the answer, called *posterior probability*. The denominator is just the summation of the numerator. Therefore, the task at this stage is to formulate the *prior probability* and the *likelihood* as the functions of F_t. There are generally two approaches to describe F_t: non-model-based and model-based approaches.

[*] The *likelihood* will be italicized in this dissertation when it indicates the likelihood of obtaining the set of the Jomon observations in this study, to distinguish it from other likelihoods.

A non-model-based approach divides age range into *m* categories, and describes F_t as a *m*-dimensional vector, $F_t = (\pi_{1t},....,\pi_{xt},....\pi_{mt})$, where $\sum_{x=1}^{m} \pi_{xt} = 1$. This approach is preferred by Caussinus and Courgeau (2010) and Séguy et al. (2013). A merit for this approach is that any F_t can be described if *m* is increased. A demerit is that the number of parameters tends to be large (=*m*−1). Additionally, as a trade-off for the versatility, the competing hypotheses must include a number of biologically unlikely hypotheses, and posterior probability will be allocated to such hypotheses regardless of the biological plausibility. For example, age-at-death distributions in which mortality decreases with age even in senile age range are included among the competing hypotheses. Although reasonable prior probability distributions could preclude such unusual hypotheses, I did not adopt this non-model-based approach for this study due to the difficulty to find such reasonable prior probability distributions for Jomon people.

A model-based approach describes the age-at-death distributions by using parametric models developed in fields of demography or fields of operating-time tests for industrial manufactures. Wood et al. (2002) introduced some mortality models including Gompertz, Gompertz-Makeham, Silar, and Weibull models to the field of paleodemography. The merit of using these models to describe F_t is that the number of parameters to be estimated is relatively small. The demerit is that they are just approximations of the real distributions in nature; for example, the Gompertz model can not describe any age-at-death distribution with two or more peaks. However, they can preclude an amount of biologically unlikely F_t's, and further preclusion is possible by confining the range of parameters and/or applying appropriate prior distributions for the parameters with rather simple biological considerations. In this study, therefore, the model-based Bayesian approach is adopted for the estimation of Jomon age-at-death distribution and will be discussed in Chapter III and IV.

Maximum likelihood approach

On the other hand, the maximum likelihood approach has also been suggested and utilized in estimation of age-at-death distributions of unearthed skeletons (Holman et al., 2002; Konigsberg and Franken-

berg, 2002; Konigsberg and Herrmann, 2002; Herrmann and Konigsberg, 2002). The maximum likelihood approach seek parameters (in this case, F_t) which maximize the likelihood function. F_t can be either non-model-based or model-based. Likelihood function is defined as a function of F_t,

$$L(F_t) \propto \Pr(y_1,....,y_n \mid F_t), \tag{1.3}$$

where $L(F_t)$ is a likelihood function and other characters denote the same in equation (1.2) and (1.3). As equation (1.3) indicates, $\Pr(y_1,....y_n \mid F_t)$ multiplied by any value which is constant with respect to F_t is considered as a likelihood function. Theoretically, the result of this method (say, F_1) is identical to the mode of the Bayesian posterior distribution by applying an uniform prior distribution which is non-zero for F_1; because, in equation (1.2), if $\Pr(F_t)$ is uniform, $\Pr(F_t)$ in the denominator comes out of the summation and cancels with that in the numerator leaving a likelihood function alone. Therefore, I consider that the maximum likelihood approach is just an aspect of Bayesian approaches. The maximum likelihood approach, however, will be used in Chapter III to compare the estimate for the Jomon life expectancy with that of Kobayashi (1967).

Summary

Age estimation by inverse regression is to be influenced by age distribution of the reference skeletons. With young-adult-dominant reference skeletons being a factor, the life expectancy at age 15 estimated by Kobayashi (1967) for Jomon people (16.1 years for males and 16.3 years for females) is probably too short. To circumvent the problem, the maximum likelihood approach or model-based Bayesian approaches will be used in the following chapters to estimate the life expectancy of Jomon people.

Chapter II

The dental pulp volume ratio as an age indicator

In this chapter, I introduce the reduction of dental pulp volume as the age indicator for Jomon skeletons. After presenting an advantage of it and reviewing the previous studies, I report the observations on 363 lower canines from recent-modern Japanese of known age and sex. Since, the morphological variation could cause undesired biases in the reduction pattern, only one tooth type was exclusively used (the lower canine). Then, I propose a statistical model to describe the observed aging pattern of the reduction. This model will be used to calculate the *likelihood* function in the following chapters.

Introduction

The Tooth as an age indicator

In the field of paleodemography, there is a long-lasting problem recognized by many researchers, which is differential preservation of skeletons regarding the age-at-death. When the recovery rate prefers young skeletons to old ones, the reconstructed age distribution based on them is younger than the true age-at-death distribution, no matter how accurately the ages are estimated. In a healthy bone, osteoblasts and osteoclasts are acting in an opposing manner renewing the bone substances; this is called bone remodeling. A reduced secretion of sex hormones in senior ages declines the activity of osteoblasts and makes the bone fragile. Presumably, this phenomenon causes the differential preservation with certain magnitude. However, since no remodeling happens in teeth (except for pathological cases), it is likely that the endurance of teeth through the taphonomical degeneration is less dependent on age than that of bones. Although using a tooth as the age indicator reluctantly preclude the people who survived without the teeth, this effect can be countered by examining the frequency of jaws with closed alveolus in the population (this will be discussed in Chapter III). Walker et al. (1988) reported significant inconsistency between the age distribution of skeletons and burial records in a mission cemetery. Although their study had some dubious

points in the skeletal age estimations and the coverage of the excavation, there might have been a significant magnitude of the differential preservation. I expect the effect of differential preservation was minimized in this study by using teeth as the main age indicator.

Pulp volume reduction by secondary dentin development

As the secondary dentin grows gradually on the wall of pulp cavity throughout life, the volume of the pulp cavity reduces with age. Today, appositional dentine tissues are distinguished into 3 types of dentin—primary, secondary, and tertiary dentin—differentiated by the time and the causes of formation as well as their histological differences. Primary dentin is formed before tooth maturation and constitutes the most volume of the tooth. After tooth eruption and root maturation, odontoblasts (dentin-secreting cells) reduce the rate of dentin formation but still physiologically continue to form dentin. This dentin is called secondary dentin. Tertiary dentin is generated as a protective reaction of the dentin–pulp complex against pathological stimuli such as caries lesion, dentin exposure by attrition and/or inflammation of pulp tissue. When dentin is exposed to oral cavity by caries, attrition or any other traumas, tertiary dentin develops and fills dentin tubules preventing bacterial intrusion into the pulp tissue.

The use of secondary dentin development as an age indicator started as early as in 1950 by Gustafson. He used ground sections of teeth and microscopes to assess the secondary dentin developments. A half century later, Kvaal and Solheim (1994) used radiographs for the assessment. Since secondary dentin is difficult to distinguish from other types of dentin on a radiograph, they measured the size of pulp cavity and assessed the degree of shrinkage to represent the secondary dentin development. Meanwhile, with the development of new computed tomography (CT) technology, the pulp cavity and the tooth have started to be measured in three-dimensional space (Vandevoort et al., 2004; Yang et al., 2006; Someda et al., 2009; Aboshi et al., 2010; Star et al., 2011). In these studies, the pulp volume ratio was calculated as pulp/tooth volumes based on the measurements on CT imageries and proposed as the age indicator. However, the numbers of samples they used were relatively small. I collected a relatively large number of lower canines and examined the pulp volume ratio on imageries taken by the CT scans. The lower canine was selected on

account of the relatively large size and simple shape of its pulp cavity and relatively long retention in the life, compared to the other types of tooth.

The time of root apex completion for lower canine is, approximately, 10–16 years of age for males and 9–14 for females (Moorrees et al., 1963). Thus, the pulp volume reduction in lower canine can be used as an age indicator only for those above these age ranges. Therefore, I limited the observations onto the Jomon samples whose age seemed to be 15 years of age or older as did Kobayashi in 1967. Following this, the samples from recent-modern Japanese were also limited to those of 15 years of age or older. Using samples from 363 individuals of known age and sex, I propose a statistical model to describe the reduction of the pulp volume ratio, in order to enable the *likelihood* calculation in Bayesian and maximum likelihood approaches in the following chapters.

Materials and methods

Japanese lower canine samples

Only one side was collected from an individual. The side in the better condition (e.g., less caries, less wear, less postmortem damage) was chosen when both sides were available. The total number of the studied individuals was 363 (209 males and 154 females). All specimens were presumed to be Japanese based on the accompanying records. The gender and the age distribution is shown in Table 1. Of all samples, 128 teeth were from individual skeletons stored in the University Museum, the University of Tokyo (UMUT), which had been cadavers in between 1880s and 1920s. Other 168 teeth were from collections of individual dentition stored in UMUT, which had been also cadavers in between 1940s and 1950s. The remaining 67 teeth were specimens prosthetically extracted from patients who had visited the hospital of the School of Dentistry at Matsudo, Nihon University since the 1970s. I used the following sampling criteria:

(1). The recorded age should be ≥15 years.

(2). The tooth should be sufficiently mature; The volume proportion of pulp canal (excluding branches) in 5mm apical root portion should be ≤ 0.09. (This criterion was made to reduce the large variation of pulp volume ratio around the time of root completion.)

(3). Lesion (due to caries, postmortem damage, etc.) should not reach the pulp cavity in the root portion.

(4). The tooth should not show a large volume loss (≥1/10 judged by visual appearance) in the root portion.

(5). The identification of lower canine should be confirmed. It should not be collected if skeptical. (This was often the case, for example, when facing complete loss of the crown part or morphological abnormality, etc.)

CT scan and image processing

To measure the volume of pulp cavity and tooth, each tooth was fully scanned by microfocal CT (micro-CT). Two micro-CT scanners were used: TXS225-ACTIS (TESCO Corporation, Tokyo, Japan) or SkyScan1173 with reconstruction software NRecon (Bruker-microCT, Kontich, Belgium). The size of element cubes (voxel size) in the reconstructed imagery was equilaterally 0.028 or 0.030 mm, respectively.

Each three-dimensional imagery was further processed using image processing software, Amira 5.2.2 (VSG, Burlington, USA). Before starting tissue segmentation, the voxel size was doubled (i.e., to 0.056 or 0.060 mm) just for data processing efficiency. Then, the imageries were segmented into *air*, *enamel*, *dentin*, and *pulp cavity*, based on the CT numbers of those voxels following the half-maximum-height procedure (Spoor et al., 1993). Opening and smoothing processes were used to remove artificial or unnecessary projection on tooth surfaces, although those were not used for the boundary between dentin and pulp cavity. Cementum was included in *dentin* as their CT numbers were too close to each other to separate them. Denticles, the calcified particles occasionally appear in pulp tissue, were included in *pulp cavity*. Dental calculus was eliminated (i.e., included in *air*) by using half-maximum-height or manual segmentation.

Secondly, the longitudinal axis for each tooth was determined as the line which bisects the major part of the root (root excluding roughly ⅓ apical tip) into right and left side equally as viewed from both labio-lingual and mesio-distal aspects. The horizontal plane was defined as any flat plane which is perpendicular to the longitudinal axis. After defining the orientation, each segmented tooth imagery was separated into two (coronal and root) portions by the horizontal plane at the height of apical-most point of cementoe-

namel junction. The coronal portions are prone to external factors that affect the pulp volume ratio, such as tertiary dentin deposition by external stimuli and tooth volume loss by dental wear or caries. To minimize those biases, coronal portions were eliminated from the volume measurement. Thus, only root portions were used for the further analyses. However, for exceptional 5 specimens in which tertiary dentin occupied the pulp cavity of the above-defined coronal portion completely, the horizontal plane between the coronal and root portions was re-defined at the most-coronal point of the *pulp cavity* in order to more preferably eliminate the effect of the tertiary dentin (Figure 3).

Third, I measured the volumes of interest by counting the voxels and then calculated pulp volume ratio in the root portion (hereafter, PVRrt). It was defined as “the volume of pulp cavity” divided by “the volume of root.” “The volume of pulp cavity” was the volume of *pulp cavity* within the root portion. “The volume of root” was the volume of *dentin* within the root portion plus “the volume of pulp cavity.”

For 24 samples where it was impossible to extract the tooth from the jaw, I scanned each of them with the jawbone. In this case, segmentation was necessary to remove bone matrices from *dentin*. The CT numbers of bone and dentin were so close that I needed manual segmentations with extra applications of smoothing functions.

In another 8 cases, with postmortem chipping-offs on the root portions, the missing parts were filled in the CT imageries by interpolating between the two unaffected image slices that bound together the affected parts. The resulted gains in the dentin volumes were no more than 5.59% of the root volumes.

Although the definition of the longitudinal axis was a bit vague, PVRrt value is not radically skewed by arbitrary choice of the axis. Indeed, when the longitudinal axes of randomly chosen 5 samples were tilted 10 degrees to random directions, PVRrt values as defined above did not change more than 2.6%.

Analyses

To confirm that PVRrt reduces with age, samples were divided into 7 age classes (15–19, 20–29, 30–39, 40–49, 50–59, 60–69, and ≥70 years), and the mean PVRrt in each class was calculated according to sex. The differences between the neighboring classes were tested by Student’s *t*-tests. Sex difference

was also tested in each age class.

A statistical model was fitted to the Japanese PVRrt values. The description of the model is the followings. PVRrt distribution conditional on age was assumed to be normal and was expanded for whole age range, where the mean of the normal distribution ($M(x)$) should follow an exponential curve as age x varies. I created 3 parameters to specify the exponential curve: A determines the shape of the curve ($A<0$), B determines parallel translation toward age-axis, and γ determines parallel translation toward PVRrt-axis. Thus, the function is written as

$$\begin{aligned} &M(x)=\exp[A\cdot(x-B)]+\gamma, \\ &M(x)=0, \text{ when } \exp[A\cdot(x-B)]+\gamma<0 \end{aligned} \tag{2.1}$$

Letting D denote the $M(15)$ (i.e., the mean initial PVRrt value), B can be expressed as $B=15-\ln(D-\gamma)^{\frac{1}{A}}$. Then, equation (2.1) becomes,

$$\begin{aligned} &M(x)=(D-\gamma)\exp[A\cdot(x-15)]+\gamma, \\ &M(x)=0, \text{ when } (D-\gamma)\exp[A\cdot(x-15)]+\gamma<0. \end{aligned} \tag{2.2}$$

As age goes to infinity, the function value $M(x)$ approaches γ (when $\gamma\geq 0$, otherwise it becomes 0), indicating γ as an asymptote for the exponential curve. These 3 parameters (A, γ, D) plus the standard deviation of the normal distribution around the curve, S (it was assumed to be constant across whole age range), describe the probability density of PVRrt (y) being y' conditional on age (denoted as $l(y=y'|\,x)$) as,

$$\begin{aligned} &l(y=y'|\,x)=\frac{1}{\sqrt{2\pi}\cdot S\cdot q}\exp\left[-\frac{1}{2}\left(\frac{y'-M(x)}{S}\right)^2\right] \\ &l(y=y'|\,x)=0 \quad (\text{when } y'>1 \text{ or } <0), \end{aligned} \tag{2.3}$$

where $q=\int_0^1 \frac{1}{\sqrt{2\pi}\cdot S}\exp\left[-\frac{1}{2}\left(\frac{t-M(x)}{S}\right)^2\right]\cdot dt$. The normal distribution was truncated as seen in equation (2.3) since the probability of PVRrt being >1 or <0 is 0. A and D were shared by males and females while γ and S were set to vary between males and females (γ_m, γ_f, S_m, S_f). Thus, total of 6

parameters ($A, \gamma_m, \gamma_f, D, S_m, S_f$) were determined at once by the maximum likelihood method, fitting the model (which now contain two exponential curves for both sexes) to the observed data.

In order to assess the goodness of fit, I tested normality of the distributions and uniformity of the variances through the age range, for males and females separately. For the normality, the distributions of residuals (signed distances of observed PVRrt values from the fitted exponential curves) were tested by Kolmogorov–Smirnov test. For the variance uniformity, the square of those residuals were tested by Kruskal–Wallis test among the above mentioned age classes.

Computer software packages, R 2.13.0 (R Development Core Team, 2011) and MATLAB (R2010b) (MathWorks, Natick, USA) were used for statistical tests and mathematical computations.

For all statistical tests, I set the significance level at 0.05.

Results

The means of PVRrt and the test results among age and sex categories are shown in Table 2. Generally, PVRrt decreased with age for both sexes. Nevertheless, decrease after age 50 was not recognizable for male. While there was no significant difference between sexes in young age classes (15–19, 20–29, and 30–39), female values tended to be significantly lower than the males in the older age classes (above 40, except 50–59).

On Figure 4 is the result of fitting the exponential-curve model to the observed data. Those parameters resulted from the fitting were summarized in Table 3. Scatter plots of the residuals against age and their distribution histograms are shown in Figure 5. Kolmogorov–Smirnov test did not reject the hypothesis that the observations of the residuals followed the normal distribution with mean = 0 and s.d. = sample s.d., for both sexes (P = 0.28 for males, 0.98 for females). Kruskal–Wallis test did not indicate significant inequality in the residual variation among those age classes, for both sexes (P = 0.08 for male, 0.41 for female). The nearly significant result of male seemed mainly caused by relatively large variation in the class of 15–19 as P value became 0.41 when that class was eliminated from the test. The variations (calculated as

$\sqrt{\frac{1}{n}\sum(residual)^2}$) for each age-class are shown in Figure 5 in parentheses.

Discussion

The analysis among age and sex categories indicated that there is a difference in the PVRrt decreasing rate between males and females. In females, the value decreased more rapidly than in males. One can also recognize this tendency by referring to the scatter diagram and the fitted curves in Figure 4. Although the reason for the difference is not clear, it could be because of some direct or indirect factors. Plausible direct factors include differences in the tooth shape and size, which influence the number of odontoblasts per root volume, or differences in gene expression of odontoblasts, which affect the degree of dentin secretion. Indirect factors include differences in hormonal homeostasis, oral environment, and masticatory stresses. The existence of the sexual difference entails the need to assess the sex composition of Jomon population when applying the PVRrt reduction model to the *likelihood* calculation. Nevertheless, to make the structure of calculations and assumptions in the *likelihood* function as simple as practical, I did not treat the sexes separately for Jomon people in this study. Therefore, the composition of sexes in Jomon population was regarded as 50% and 50% at any age, and will be so in all the following chapters. Details about the *likelihood* calculation will be discussed in Chapter III.

Although the test for uniformity of the variation of PVRrt fell close to the significance level in males (*P* value =0.08), variation along the model curve was treated as constant in this study. While the statistical model I adopted may not thoroughly describe the nature of PVRrt reduction, I supposed that the model was good enough to approximate the probability distribution of PVRrt. The reason why teen-age samples had relatively large variation might be attributed to the difference in the initiation time of odontogenesis. A slight difference of the time should cause large difference when PVRrt reduction is still rapid.

In this chapter, the values of the parameters ($A, \gamma_m, \gamma_f, D, S_m, S_f$) were determined. In the following chapters, those values will be used in the *likelihood* calculation except of γ_m and γ_f. The reason not to use them is to take into account the possibility that the reduction rates of PVRrt may be different

between recent-modern Japanese and Jomon people. The value of the parameter (denoted as a single parameter, γ, as sexes are combined in Jomon people) is to be estimated by Bayesian theorem simultaneously with F_t, the age-at-death distribution of Jomon people. In the frame of Bayesian theorem, there is no limitation in the number of parameters to be estimated. Although one has to be parsimonious about the number of parameters to keep the estimation practical, there is no reason to limit the parameters to those describing the age-at-death distribution.

Summary

As an age indicator, I adopted the pulp volume ratio in the lower canine. In this chapter, its reduction with age was confirmed in the recent-modern Japanese samples. The probability density conditional on age was parameterized with an exponential-curve model, and values for the parameters were determined by fitting the model to the Japanese data. The model and the values will be used in the *likelihood* calculation for the maximum likelihood approach in Chapter III, and for the Bayesian approaches in Chapter IV.

Chapter III

Maximum likelihood approach and the comparison with the life expectancy by Kobayashi (1967)

In this chapter, an estimate of life expectancy at age 15 (e_{15}) of Jomon people is calculated by the maximum likelihood approach based on the information from 234 Jomon samples. Then, I compare the estimate with that of Kobayashi (1967) and test the difference by simulating e_{15}'s upon a null hypothesis that the 234 samples are outcomes from the age-at-death distribution estimated by Kobayashi (1967). The result shows that the estimate of e_{15} from the real samples lies significantly older than the distribution of e_{15}'s upon the null hypothesis.

Introduction

In Chapter I, one reason was discussed why the estimate of Jomon life expectancy by Kobayashi (1967) should have been too young, and Bayesian and maximum likelihood approaches were suggested to circumvent the problem. In order to conduct either approach, the *likelihood* function should be introduced. The *likelihood* function comprises multiplication of the probability densities for all the Jomon individuals observed in this study. Thus, the main task is to describe the probability (density) of obtaining the observation for each individual. The statistical model to describe the probability density of obtaining a PVRrt value was parameterized in Chapter II. Nevertheless, further observations were needed to apply the model to the Jomon samples. The majority of the following *Materials and methods* section is devoted to explanations for the statistical models to describe the probability of obtaining those observations. Those models are the followings:

(1). In order to describe the probability density for an individual being at certain age before any observations, a model for the age-at-death distribution developed in the field of demography was introduced.

(2). The above age-at-death distribution has to be calibrated for correcting a gap between the age distri-

bution of the lower-canine samples and the true age-at-death distribution. This is because the collection of lower-canines does not include the people who survived without lower-canines. For the calibration, a model was devised to describe the age-specific probability of lower-canines to be missing in an individual.

(3). The PVRrt reduction model has to be modified into that with 50:50 sex ratio, as gender was disregarded for the Jomon samples.

(4). Among the individuals with the lower-canine observation, epiphyseal closure was assessed at the sternal end of the clavicle, in order to complement the age information obtained from the PVRrt observation. For this, a model was provided to describe the age-specific probability of the epiphyseal closure being completed.

(5). The observation on the clavicle entails the need to take into account the probability for existence of the clavicle(s) (i.e., the availability for the clavicle observation) if this probability depends on age. A model was utilized to describe the probability.

After the description for the Jomon materials used in this study, those five models are explained in detail in the following section. Then, the method to calculate the *likelihood* function is explained combining those models. At the end of the section, I describe the statistical approach used to test the difference in the results between the maximum likelihood approach and Kobayashi (1967).

Materials and methods

Jomon materials

The Jomon samples used in this study were drawn from the skeletal collections stored in UMUT. I examined all the collections thoroughly as much as possible in search for lower canines. Samplings were conducted so as not to sample both of the two lower canines from an individual. When the tooth was not accompanied by the corresponding jaw bone, careful attention was paid for erroneous sampling; every isolated lower canine was checked to see if it could be the opposite side of an already collected one to avoid redundancy. Only lower canines with a proof against the possible antemortem tooth loss were col-

lected as the sample. As in Kobayashi (1967), only specimens whose age seemed to be 15 years or older were considered. Lower canines with immature roots whose apex still opened, or those with immature pelvis whose primary elements remained completely separated were not collected. The sampling criteria (2)–(5) in Chapter II were also applied here. Only one sample was eliminated by the criterion (2). Some were precluded by the criteria (3)–(5). Additionally, I had to care about an intentional tooth extraction—or tooth ablation—habit in Jomon society. Intentional extraction for anterior dentition was common in several localities during the Late to Final Jomon periods. If this habit had been prevailing in the locality where the samples come, the lower canine samples would have been biased being younger than the reality. To avoid this effect, all samples from the site with intensive lower-canine ablation were eliminated. How to judge whether the habit had been intensive will be discussed later. Eventually, lower canine teeth from 234 Jomon individuals were collected. The locations of the archaeological sites for the Jomon individuals are mapped in Figure 6. Distribution of the individuals according to the Jomon sub-periods is shown in Figure 7. CT scans, the image segmentations, and the calculations of PVRrt values were conducted in the same manner as described in Chapter II. Out of 234, 42 samples were scanned with the mandible. The postmortem chipping-offs were filled in 7 teeth and the gains were no more than 2.43% of the root volumes. In accordance with the definition described in Chapter II, the plane between the coronal and root portions for 22 Jomon teeth was set at most-coronal point of the pulp cavity, due to the tertiary dentin development or total enamel loss.

Along with the effect of tooth ablation, possible biases due to spontaneous tooth loss should be considered. The latter case also biases the estimated age distribution being younger than the reality, because those older individuals who lived for certain period without the teeth are not included in the sample. The age-at-death distribution model has to be calibrated to that of age-at-death distribution of the people with canine(s) at their death, to properly calculate the probability for the canine-sampled individual to be at age x. For this, I need the ratio of people who died with no lower canines against all who died at or above 15 years of age. It was estimated by the following procedure. Among the collection stored in UMUT, all lower jaw bones with canine alveolar parts were examined to determine if each of the individuals had re-

tained the canine(s) at the time of death. After exclusion of those jaws judged as being below 15 by the development of teeth, etc, those with one or two socket(s) for lower canine(s) were counted as individuals died with canine. Those with closed sockets in both sides were counted as those died with no canines. For jaw bones of only either right or left side remaining, the same condition was assumed on the missing side. Attention was paid so as not to count double for right and left pieces from an individual. Socket closures due to the tooth ablation had to be eliminated, although the judgment whether the closure of socket was due to tooth ablation or spontaneous tooth loss was difficult especially for a jaw with few teeth. Therefore, I eliminated all the jaw samples from sites where the case of obvious ablation exceeded 1/3 of the total specimen in the site (intensive lower-canine ablation sites). Jaws with obvious ablation not from those sites were also eliminated. Thus, of 412 total individuals, 30 were confirmed as those died without lower canines. 30/412 gave the canine-loss ratio T_R=0.0728.

As for the samples to assess the state of completion of the epiphyseal closure at clavicular sternal ends, 55 individuals retained one or two sternal end(s) out of 234 individuals with canines. The scoring criteria were modified from those of McKern and Stewart's 5-stage system (McKern and Stewart, 1957); if the epiphysis was completely fused with no trace, it was scored as "complete," otherwise it was scored as "incomplete." No individual exhibited right-left inconsistency in the state of the closure.

The Gompertz model

To describe an age-at-death distribution (F_t), I adopted the Gompertz model. The Gompertz model has two positive parameters (α, β). This model assumes that the mortality exponentially increases with age. This can be formulated as

$$\mu(x) = \alpha \cdot \exp[\beta \cdot x], \tag{3.1}$$

where $\mu(x)$ is the mortality (or "force of mortality" to be specific) function and x is age. General human mortality profiles show a pattern where with relatively high mortality at birth, it decreases rapidly to lowest point at around the beginning of adolescence, then it increases with age in approximately exponential manners. Thus, to describe the mortality patterns after 15 years of age, the Gompertz model was con-

sidered to be appropriate.

A survival function is a function of age which describes a decrease with age in the proportion of survivors in a cohort. There is a general relation between the survival function $s(x)$ and the mortality function $\mu(x)$ described as

$$\frac{1}{s(x)} \cdot \frac{d\, s(x)}{dx} = -\mu(x). \tag{3.2}$$

Integrating this equation gives

$$\frac{s(x)}{s(x_0)} = \exp\left[-\int_{x_0}^{x} \mu(t) \cdot dt \right]. \tag{3.3}$$

The survival function generally starts with unity at the starting age x_0 (i.e., $s(x_0) = 1$). In this dissertation, the starting age is 15; therefore equation (3.3) can be written as

$$s_{15}(x) = \exp\left[-\int_{15}^{x} \mu(t) \cdot dt \right], \tag{3.4}$$

where the subscript "15" in $s_{15}(x)$ denotes that the function starts at age 15. Thus, with equation (3.1), $s_{15}(x)$ becomes

$$s_{15}(x) = \exp\left[\frac{\alpha \cdot e^{15\beta}}{\beta} (1 - e^{\beta(x-15)}) \right]. \tag{3.5}$$

Figure 8 shows the results of fitting the $s_{15}(x)$ to the reported survival data of several populations including primates. The Gompertz model generally approximates these survival data. The method used for the fittings is detailed in Appendix A.

When the stationary population is assumed (i.e., no population growth nor decline and no secular change in the mortality and fertility profiles), the age-at-death distribution in the cohort can be thought as the age-at-death distribution of the population. The age-at-death probability density function (PDF) $f_{15}(x)$ can be derived by differentiating $s_{15}(x)$ over the range $x \geq 15$.

$$f_{15}(x) = -\frac{d\, s_{15}(x)}{dx}. \tag{3.6}$$

Thus,

$$f_{15}(x) = \alpha \cdot \exp\left[\beta x + \frac{\alpha \cdot e^{15\beta}}{\beta}(1 - e^{\beta(x-15)}) \right], \qquad (3.7)$$

$$f_{15}(x) = 0, \text{ when } x < 15.$$

Now, F_t is an age-at-death distribution to be specified by the values of α and β and the probability density at any age-at-death x is calculated by equation (3.7).

The model for tooth loss

A probit function was used to model the probability of spontaneous tooth loss (i.e., tooth loss due to senescence). A probit function describes the probability that an event was already happened to a person, based on an assumption that the time of the event (which happens once in a life) distributes normal in the population. In many cases, log-normal distribution is used instead of normal distribution, since normal distribution allocates a probability to negative age. Log-normal distribution becomes the normal distribution when the logarithm is applied on age. Here, I assumed that the occurrence of the total loss of lower canines distributes log-normal. Let w be a categorical variable which comes out either "lost" or "retained." Thus, the probability of w being "lost" is a function of age x, described as

$$\Pr(w = "lost" | x) = \int_0^x \frac{1}{t\sqrt{2\pi} \cdot T_S} \exp\left[-\frac{1}{2}\left(\frac{\log(t) - T_M}{T_S} \right)^2 \right] \cdot dt, \qquad (3.8)$$

where T_M and T_S are the parameters of log-normal distribution. These can be regarded as the mean and s.d., respectively, of the normal distribution when applying logarithm on age. The relation between (T_M, T_S) and (mean, s.d.) of the log-normal distribution is

$$mean = \exp\left[T_M + \frac{{T_S}^2}{2} \right], \quad s.d.^2 = \left(\exp\left[{T_S}^2 \right] - 1 \right) \cdot \exp\left[2T_M + {T_S}^2 \right]. \qquad (3.9)$$

In the report of dental survey as of 2005 by Ministry of Health, Labour and Welfare (undated), data about the presence of lower canine teeth according to age classes are available (data from Japanese). I fitted the log-scale probit model to the data by a maximum likelihood method. Male and female data were combined before the fit. Only right lower canine data were used. Details about the method to fit is in Ap-

pendix B. The result of the fit is shown in Figure 9. T_M was 4.4459 and T_S was 0.2530. Corresponding mean and s.d. are 88.0 and 22.6 years. I assumed the T_S to be the same between the Japanese and Jomon people. Although these parameters are for the distribution of the time of *right* lower canine loss, not of *total* lower canine loss, I assumed in this study that T_S =0.2530 was an approximation of that of total lower canine loss in Jomon people. To determine T_M for Jomon people, the canine-loss ratio T_R =0.0728 was used. When it is assumed that the risk of death is unchanged by whether the person has the teeth or not, then, the canine-loss ratio can be described with $f_{15}(x)$ as

$$T_R = \int_{15}^{\infty} \Pr(w = "lost" \mid x) \cdot f_{15}(x) \cdot dx . \tag{3.10}$$

This equation contains variables T_R, T_M, T_S, α, and β. Here, T_S is a constant = 0.2530 as mentioned above. Since we have the canine-loss ratio T_R =0.0728, T_M can be described as function of α and β, provided that one and only one T_M is specified by the T_R (regarding α and β as constants). This condition is satisfied, because as T_M increases from $-\infty$ to $+\infty$, T_R decreases monotonically from 1 to 0, specifying one and only one T_M which correspond to the T_R =0.0728. In other words, the later the mean time of tooth loss (described in equation (3.9) with fixed T_S) occurs, the smaller proportion the people without canines occupies in the population. Although equation (3.10) can not be solved algebraically for T_M, it can be done computationally. Now, T_M is regarded as a function of α and β.

The model for PVRrt reduction

The model for PVRrt reduction established in Chapter II was sex-specific. As mentioned, I did not separate the sexes of Jomon samples and assumed 50:50 sex ratio in the whole age range of Jomon people. To describe the PVRrt reduction of Jomon people with single exponential model, the sex-specific parameters determined in Chapter II have to be combined. The parameters determined were ($A, \gamma_m, \gamma_f, D, S_m, S_f$). γ does not have to be combined since it represents the rate of PVRrt reduction and thus was treated as one of the unknown parameters in Jomon people. S_m and S_f has to be

combined to give s.d. along the single Jomon PVRrt reduction curve, assuming 50:50 sex ratio (S). When (M_m, S_m) and (M_f, S_f) are mean and s.d. of two probability distributions, the mean (M) and s.d. (S) of the combined distribution (assuming 50:50 ratio) are calculated as

$$\begin{aligned} M &= \frac{M_m + M_f}{2}, \\ S^2 &= \frac{S_m^2 + S_f^2}{2} + \frac{(M_m - M_f)^2}{4}. \end{aligned} \tag{3.11}$$

In the case of PVRrt reduction, as $M_m - M_f$ vary with age, S also varies with age. Since the two exponential curves separate more as age increases, S increases with age. The resulting combined distribution was also assumed to be normal. As a summary, the parameters (A, D, S) were considered as the same between recent-modern Japanese and Jomon people. However, γ for the Jomon people was remained to be estimated.

The model for the epiphyseal closure at the sternal end of clavicle

The γ in the PVRrt exponential curve model is the asymptote of the curve when age goes to infinity. With the γ being unfixed in the calculation of the *likelihood* function, the information from the PVRrt observations is insufficient to determine α and β with decent precision. Therefore, it was needed to restrain γ within a plausible range. This becomes possible through referring to the clavicular epiphyseal closure. The sternal epiphyseal closure of the clavicle completes at around late 20s of age. Imagine that the occurrence of the closure event was corresponding to around 0.05 of PVRrt value in the Jomon samples, then, the exponential curve of PVRrt reduction has to pass the area around the intersection of late 20s and 0.05 of PVRrt, narrowing the possible range for γ (Figure 10).

To include the information of clavicles in the *likelihood* function, the probability of the closure being completed has to be modeled. Langley-Shirley and Jantz (2010) used the log-scaled probit model to describe the probability based on the clavicles from total of 1289 individuals. Letting z^{fuse} be a categorical variable which comes out either 1 or 0 denoting “complete” or “incomplete,” respectively, the model can

be described in the similar way as in equation (3.8). That is

$$\Pr\left(z^{fuse}=1\mid x\right)=\int_0^x \frac{1}{t\sqrt{2\pi}\cdot U_S}\exp\left[-\frac{1}{2}\left(\frac{\log(t)-U_M}{U_S}\right)^2\right]\cdot dt\,, \tag{3.12}$$

where U_M and U_S are parameters of the log-normal distribution which are equivalent to T_M and T_S in equation (3.8). In their reported data using Hamann–Todd collection (n=354), they are U_M =3.329 and U_S =0.1133 for males, and U_M =3.233 and U_S =0.1222 for females. (They used 3-phase scoring system: "None," "Fusing," and "Fused." These numbers are the log-probit parameters describing the last transition, "Fusing–Fused.") The male and female parameters were, then, combined by using equation (3.11) to apply them to Jomon people, resulting U_M =3.281 and U_S =0.1273 (corresponding mean and s.d. of the age are 26.8 and 3.43 years, respectively). This implies an assumption that the mean and s.d. for age of the closure are the same between Hamann–Todd collection (62% European American and 38% African American) and Jomon people.

The model for the probability to retain a clavicle conditional on retaining a canine

In whole of this dissertation, it is assumed that the probability for a tooth to survive the taphonomic processes is independent of age. However, the survival of a clavicle is more likely to depend on age than teeth, since bone remodeling activity decreases through the life. When the chance to survive is different with age, it has to be taken into account in the *likelihood* function. Since examined clavicles were only those of individuals with their lower canines, what should be considered here is the probability of retaining one/two clavicle(s) conditional on a lower canine being retained already. Here, I assumed a linear model which is described as

$$\begin{aligned}
&\Pr\left(z^{prsv}=1\mid x\right)=\lambda+\theta\cdot(x-15)\,,\\
&\Pr\left(z^{prsv}=1\mid x\right)=1,\quad \text{when}\quad \lambda+\theta\cdot(x-15)>1,\\
&\Pr\left(z^{prsv}=1\mid x\right)=0,\quad \text{when}\quad \lambda+\theta\cdot(x-15)<0\,.
\end{aligned} \tag{3.13}$$

where z^{prsv} is a categorical variable which comes out either 1 or 0 denoting "retained" or "lost," respectively, and, λ and θ are the parameters to be estimated. That is, λ denotes the probability of one/two

clavicle(s) to be retained for an individual (with canine(s)) of age 15, and θ denotes the slope of the change with age. Although it is skeptical that the probability for retaining a clavicle changes linearly with age, this assumption is better than not considering any change with age.

Combining those models to calculate the likelihood function

Now that all models to be used in the calculation were described, I explain how to calculate the *likelihood* function. I mentioned earlier that a likelihood function is a function which is proportional to the probability to obtain the set of observations $y_1,....,y_n$ conditional on certain age distribution F_t. Letting y_i denote the PVRrt value for individual i, the word "probability" should be replaced by "probability density," since PVRrt is a continuous variable. Furthermore, the observation is, now, not only on PVRrt values but also on the epiphyseal closure and the preservation of the clavicle. For these, let z_i denote the set of the three observations ($z_i = \left(y_i, z_i^{fuse}, z_i^{prsv}\right),\ i = 1,2,3,....,234$). And, as the parameters to be estimated are not only for F_t but also for other statistical models, let Ω denote the set of $\alpha, \beta, \gamma, \lambda$ and θ.

The probability density for an individual with canine(s) being x_i years old (x is also considered to be a continuous variable, here) is

$$p(x = x_i \mid \Omega) = \frac{f_{15}(x_i \mid \alpha, \beta) \cdot \left(1 - \Pr(w = "lost" \mid x_i, \alpha, \beta)\right)}{\int_{15}^{\infty} f_{15}(x \mid \alpha, \beta) \cdot \left(1 - \Pr(w = "lost" \mid x, \alpha, \beta)\right) \cdot dx}. \tag{3.14}$$

Assuming the independence between PVRrt and the closure completion at fixed age, the probability density that $z = z_i$ *when* the individual is x_i years old is

$$\begin{aligned} p(z = z_i \mid x_i, \Omega) = l(y = y_i \mid x_i, \gamma) \\ \cdot \left[\Pr\left(z^{fuse} = 1 \mid x_i\right)\right]^{z_i^{fuse} \cdot z_i^{prsv}} \cdot \left[1 - \Pr\left(z^{fuse} = 1 \mid x_i\right)\right]^{(1 - z_i^{fuse}) \cdot z_i^{prsv}} \\ \cdot \left[\Pr\left(z^{prsv} = 1 \mid x_i, \lambda, \theta\right)\right]^{z_i^{prsv}} \cdot \left[1 - \Pr\left(z^{prsv} = 1 \mid x_i, \lambda, \theta\right)\right]^{(1 - z_i^{prsv})}. \end{aligned} \tag{3.15}$$

This equation is the multiplications of equations (2.3), (3.12), and (3.13). Thus, the probability density that $z = z_i$ *and* the individual is x_i years old is the multiplication of equations (3.14) and (3.15):

$$p(z = z_i, x = x_i \mid \Omega) = p(z = z_i \mid x_i, \Omega) \cdot p(x = x_i \mid \Omega). \quad (3.16)$$

Integrating the equation (3.16) for whole age range gives the probability density of an individual being $z = z_i$. That is

$$p(z = z_i \mid \Omega) = \int_{15}^{\infty} p(z = z_i, x = t \mid \Omega) \cdot dt. \quad (3.17)$$

Since the sampling choices were independent from the outcomes of the other individuals, the probability density of obtaining $z_1,....,z_{234}$ (i.e., the *likelihood* function $L(\Omega)$) is the product of the equation (3.17). That is

$$L(\Omega) = p(Z = (z_1,..., z_{234}) \mid \Omega) = \prod_{i=1}^{234} p(z = z_i \mid \Omega). \quad (3.18)$$

Maximizing the likelihood function

To find the parameters which maximize the *likelihood* function, a calculation program equipped in MATLAB (R2010b) (MathWorks, Natick, USA) utilizing the Nelder-Mead simplex algorithm was used with random starting points.

The null hypothesis and the computer simulations

First, an estimation of the parameters Ω was determined from the 234 Jomon samples by the maximum likelihood approach. Using α and β of the estimated Ω, the life expectancy at age 15 (e_{15}) was calculated. e_{15} can be calculated as

$$e_{15} = \int_{15}^{\infty} s_{15}(x) \cdot dx. \quad (3.19)$$

Hence, ${}_{real}\hat{e}_{15}$ is used to denote the estimate from the real Jomon samples.

To statistically test the difference from the result of Kobayashi (1967), “pseudo-estimates” were generated upon a null hypothesis that the age-at-death distribution by Kobayashi (1967) is true. The Gompertz model was fitted to the age-at-death distribution in Kobayashi (1967) (sexes were combined, see Appendix

A for details). Then, the resulting α and β (denoted here as α_K and β_K) were used to computationally generate "pseudo-samples" whose ages distribute according to the Kobayashi's result. Before assigning PVRrt values to the pseudo-samples, the canine-loss ratio had to be taken into account. Thus, the pseudo-samples were culled according to the tooth-loss probability described in equation (3.8). Mimicking the 234 actual Jomon samples, 234 pseudo-samples were generated in this way. Then, the PVRrt values and the states of the claviclular closure and its preservation were assigned to the pseudo-samples according to the probability (density) described in equations (2.3), (3.12), and (3.13), respectively. To do so, however, γ, λ, and θ have to be specified. Here, γ, λ, and θ which maximize the *likelihood* function with $\alpha = \alpha_K$ and $\beta = \beta_K$ was deemed to be the most conservative values to use, with the intent of detecting the statistical difference. From the 234 pseudo-samples generated in this way, an pseudo-estimate of Ω was determined likewise by the maximum likelihood method and then the pseudo-estimate of the life expectancy was calculated. Repeating this process (from generating pseudo-samples to obtaining the pseudo-estimate) 500 times, 500 pseudo-estimates of the life expectancy (denoted as ${}_{hypK}\hat{e}_{15}$) were obtained.

Results

The observations on the PVRrt values and the states of clavicular sternal closure and its preservation for 234 Jomon samples are summarized in Figure 11. The parameters resulted from the maximum likelihood approach on the real Jomon samples is summarized in Table 4. The age-at-death distribution, and PVRrt reduction curve resulted from those estimated parameters are depicted in Figure 12. The resultant ${}_{real}\hat{e}_{15}$ was 30.6 years.

All 500 ${}_{hypK}\hat{e}_{15}$'s were smaller than the ${}_{real}\hat{e}_{15}$ (Figure 13), indicating the age distribution of the population represented by the 234 Jomon samples was significantly older than the age-at-death distribution estimated by Kobayashi (1967).

Discussion

The skeletal samples that Kobayashi used in 1967 were those stored in the Department of Anthropology of the University of Tokyo. The majority of the collection in the department are now stored in UMUT. Although identification of the samples he actually used is not possible in many cases, a number of individuals should have been included both in his study and in the present study. Out of 234 Jomon samples used here, 144 belong to the same sites as Kobayashi reported in his paper. Hence, I conclude that Kobayashi's estimates for the age distribution and the life expectancy at age 15 were too young for Jomon people. The reason for the underestimation may have been more than one. Inverse regression with young adult–dominant reference samples should have been one of them. The other reasons may include the differential preservation, since most of the age indicators he used were relatively fragile skeletal parts (such as pubic symphysis). On the other hand, age indicators only applicable to young individuals (i.e., epiphyseal unions) may have unintentionally precluded old Jomon skeletons from his observations.

Summary

Using a maximum likelihood approach, the age-at-death distribution and life expectancy at age 15 were estimated for Jomon people. The life expectancy was significantly older than that Kobayashi estimated in 1967. In the following chapter, Bayesian approaches will be used to associate probabilities to the estimates.

Chapter IV

Bayesian approaches for Jomon survival profiles

In this chapter, probable ranges of survival function and the life expectancy (e_{15}) of Jomon people are calculated using Bayesian approaches. Before the calculations, the concept of Bayesian estimation (inference) and interpretation of the answer—posterior probability—are briefly discussed. Then, I propose a prior probability distribution of the Gompertz parameters (α, β), for prehistoric populations such as Jomon people, based on the life-table data of modern and historical human populations. The results are compared between cases for different prior distributions where uniform priors were used for all parameters and where the non-uniform prior for (α, β) was applied.

Introduction

Interpretation of the posterior probability distribution

In this section, I point out that the result from the Bayesian approach has to be interpreted carefully. When the choice of the prior probability is inappropriate, the posterior probability can not be regarded as the probability of the estimating parameters. The inappropriate choices may include uniform prior distributions. One may think that a uniform prior is the appropriate prior distribution when no prior information is available. However, this is not true. Here is an example. We are now aiming to estimate the Gompertz parameters (α, β) for Jomon people. Let A be a logarithm of α and B be a logarithm of β, then (A, B) can be the parameters to specify the Gompertz model, too. Both (α, β) and (A, B) can be regarded as the parameters to be estimated by Bayesian approach. The mischief is that assuming uniform prior distributions for one makes the prior distributions for the other far different from uniform distributions. What I propose by this example is that uniform prior assumption is nothing but one of arbitrary choices for the prior.

Nevertheless, there is one point where uniform prior is special. As mentioned earlier, with uniform

prior, the prior function in the denominator in equation (1.2) cancels with that in the numerator and leaves the likelihood function alone. This implies the posterior distribution is identical to the likelihood function when uniform prior is used (provided that the range of the uniform distribution is sufficient). For hypotheses where the likelihoods are nearly zero, the posterior probabilities are also nearly zero (unless an unusual prior distribution is applied). Therefore, I suppose that the posterior probability distribution resulted from uniform priors can be interpreted as indicating the possible range (the very "rough" range such as 95% range) among the hypotheses, although the details (e.g., the mean, s.d., the "shape" of the distribution, etc.) are skeptical.

To make the posterior probability distribution credible into the details, an application of the appropriate prior probability distribution is necessary (I refer to this as "ideal prior"). In many cases, however, to find such prior is difficult. The important thing is to make the prior distribution close to the ideal prior as much as possible in light of experimental data and asses the appropriateness with empirical knowledge about the subject.

Prior probability distributions

In this study, uniform prior distributions were primarily used. The suppositions of the uniform prior distributions for those parameters of Jomon people may not be good approximations to the ideal prior probabilities. For this study, the ideal prior probability distribution would be the distributions of those parameters hypothetically achieved by a number of human population who lived under the similar environment and with similar genetic composition to those of Jomon people. Nevertheless, since no information was available to determine such ideal distribution (some information for the Gompertz parameters (α, β), at best), I reluctantly used uniform priors.

Even in this situation, some information was available about the prior probability of α and β—from modern and historical human life-table records. Life-tables show age-breakdown data for the probability of death, the number of survivors, the life expectancy, etc. calculated from the number of survivors and deaths in the period of survey. First, I collected the life-tables of human, great apes, and some

cercopithecine monkeys in search for a general relation between α and β in primates. Although such comprehensive pattern could not be found, I could detect a unique trend in human life-tables, which distinctly separated humans from the other primates. Figure 14 shows the relation between life expectancy at age 15 (e_{15}) and coefficient of variation (CV) of the years-to-death after age 15. They were calculated from α and β obtained by fitting the Gompertz model to the adult range of each life-table (see Appendix A for the details of the methods to fit). The function of (α, β) to give (e_{15}, CV) seemed a injective function, confirmed by exhaustive calculations, which means any describable (e_{15}, CV) by the Gompertz model has one and only one corresponding (α, β). In the figure, human populations show a pattern of straight line and the other primate populations are not located on the human line nor on the extension of it. This indicates that the pattern of survival curves is different between humans and other primates *in addition to* the difference in the general longevities between them. As e_{15} decreases in human group, the CV increases. If e_{15} of Jomon people should fall in a range of 20–30 years, it is plausible to say that the CV would not fall in the ape range but be larger than that. The survival profile of a human population with low level of longevity seems not to be the intermediate between humans and the great apes.

Therefore, a prior distribution was proposed for (α, β) using the distribution of human (e_{15}, CV) data. The distribution of CV conditional on e_{15} was estimated by a linear regression analysis and a uniform distribution of e_{15} was assumed. Then, this distribution was converted to that of α and β.

Materials and methods

Materials

The same data of 234 Jomon samples used in Chapter III were used. Information for the life-tables used to obtain the prior distribution is summarized in Table 5.

Calculation of the prior probability

The Bayesian theorem in equation (1.2) is re-written as

$$p(\Omega \mid z_1,....,z_n) = \frac{g(\Omega)\cdot L(\Omega)}{\int_\Omega g(\Omega)\cdot L(\Omega)\cdot d\Omega}. \tag{4.1}$$

$g(\Omega)$ is the prior probability density function (PDF). $L(\Omega)$ is the *likelihood* function described in equation (3.18), Ω is the set of the parameters to which the posterior probability densities are to be assigned (i.e., α, β, γ, λ, and θ). As (α, β) and the other parameters are regarded as independent from each other in the prior distribution, equation (4.1) is written as

$$p(\Omega \mid z_1,....,z_n) = \frac{g_{\alpha,\beta}(\alpha,\beta)\cdot g_\gamma(\gamma)\cdot g_\lambda(\lambda)\cdot g_\theta(\theta)\cdot L(\Omega)}{\int_\Omega g_{\alpha,\beta}(\alpha,\beta)\cdot g_\gamma(\gamma)\cdot g_\lambda(\lambda)\cdot g_\theta(\theta)\cdot L(\Omega)\cdot d\Omega}, \tag{4.2}$$

where $g_\bullet(\bullet)$ are the respective prior PDFs. $g_{\alpha,\beta}(\alpha,\beta)$ was calculated from the data of current and historical human populations and modern hunter-gatherers. As depicted in Figure 15, a linear regression of CV on e_{15} was calculated and the prediction distribution was assumed to be the prior distribution of CV conditional on the e_{15}. That is, it was calculated on the assumption of

$$\frac{\mathrm{CV} - \left(\frac{S_{eC}}{S_{ee}}(e_{15} - M_e) + M_{\mathrm{cv}}\right)}{\sqrt{\mathrm{V}\cdot\left(1 + \frac{1}{\mathrm{N}} + \frac{(e_{15} - M_e)^2}{S_{ee}}\right)}} \sim t(N-2), \tag{4.3}$$

where N is the number of samples, V is the square-sum of distances from the regression line divided by $N-2$, M_e and M_{cv} are the sample mean of e_{15} and CV, respectively. S_{ee} is the square-sum of the distances from M_e. S_{eC} is the covariation of e_{15} and CV. The distributions were truncated at 0 and 1, since CV<0 is impossible and CV≥1 is not describable by positive α and β. Then, the uniform distribution of e_{15} between 0–70 was assumed. This 2-dimensional PDF is in the scale of e_{15} and CV. This has to be transformed into the PDF in the scale of α and β (i.e., $g_{\alpha,\beta}(\alpha,\beta)$). Let $h(e_{15},\mathrm{CV})$ be the PDF in the scale of e_{15} and CV. This can be transformed as

$$g_{\alpha,\beta}(\alpha,\beta) = h(e_{15},\mathrm{CV})\cdot\left\|\begin{matrix}\frac{\partial e_{15}}{\partial\alpha} & \frac{\partial \mathrm{CV}}{\partial\alpha}\\ \frac{\partial e_{15}}{\partial\beta} & \frac{\partial \mathrm{CV}}{\partial\beta}\end{matrix}\right\|, \tag{4.4}$$

where $\| \ \|$ denotes the absolute value of the determinant. In practice, $\log(\alpha)$ and $\log(\beta)$ were used to intermediate the transformation to minimize the numerical error in the computation. Figure 15 (lower picture) shows the PDF in the scale of $\log(\alpha)$ and $\log(\beta)$.

Calculation of the posterior probability

Before applying the prior distribution explained above, uniform priors were applied to all the parameters. The ranges of the uniform distributions were [0–1], [0–1], [−0.05–0.05], [0–1], and [−0.1–0.1] for α, β, γ, λ, and θ, respectively. Next, the "non-uniform" prior distribution was applied to α and β. For the other parameters the same uniform priors were used. The calculation of equation (4.2) requires 5-dimensional integration, which was computationally highly demanding. Thus, Markov chain Monte Carlo (MCMC) method was used with Metropolis–Hastings algorithm. MCMC method can create a chain of random samples which distribute according to any requested probability distribution function of a number of dimensions. I created 48,000 random samples by MCMC for each case. Marginal posterior distributions of the parameters, a posterior distributions of life expectancy at 15, and credible intervals* of the survival curve were calculated from those random samples. To obtain the maximum point (the mode) of the posterior distribution, Nelder-Mead simplex algorithm was used. MATLAB (R2010b) (MathWorks, Natick, USA) was used for those mathematical computations.

Results

The sample variance-covariance matrix resulted from the regression is shown in Table 6.

The marginal posterior distributions of parameters when uniform priors were used for all of them are shown in Figure 16. Means, medians, and 95% credible intervals of the marginal distributions are summarized in Table 7. The mode of the posterior distribution (not marginal) is the same as the result of maxi-

* Credible interval is a term of Bayesian inference. X% credible interval was defined in this dissertation as the interval between (100−X)/2 percentile and 100− (100−X)/2 percentile values of the posterior probability distribution.

mum likelihood approach in Chapter III. The posterior distribution of e_{15} calculated from the random samples is shown in Figure 17. The mean was 29.50 years and the 95% credible interval was 19.45–43.60 years. The survival curve calculated from the mode and the 95% credible interval of the curve passage are shown in Figure 18 with comparisons to the curves of some other populations. The marginal posterior distributions of parameters when non-uniform prior was applied to (α, β) are shown in Figure 19. Means, medians, and 95% credible intervals for the marginal distributions are summarized in Table 8. The mode of the posterior distribution (not marginal) is shown in Table 9. The posterior distribution of e_{15} is shown in Figure 20. The mean was 35.19 years and the 95% credible interval was 29.19–41.52 years. The survival curves are shown in Figure 21 in the similar manner as in Figure 18.

Discussion

Age-dependent change in taphonomical endurance θ and PVRrt reduction rate γ

Judging from the credible intervals of θ, preservation of clavicles relative to that of teeth seemed not to change significantly with age, although the means and the modes were all negative in the results of both prior assumptions. The age-dependence of bones in taphonomical endurance was not evident in this study, but the negative tendency in the posterior distributions of θ was suggestive for its existence.

The posterior distributions of γ indicate that γ for Jomon people was significantly lower than that of recent-modern Japanese of any sex. PVRrt value seemed to have reduced more rapidly in Jomon people than does it in recent-modern Japanese. As the exact cause is unknown, the explanations will be the same as those in Chapter II for the sex difference in Japanese samples. In addition, however, since the degrees of attrition are obviously different between the two populations, the external stimuli might have influenced the rate of dentin development, despite the elimination of coronal portion to avoid such effect. On the other hand, the difference in tooth size may be another candidate for the explanation. The root volumes were different between the Jomon and the Japanese samples (Jomon<Japanese, $P<0.01$ by *t*-test). This is consistent with the measurements of crown dimensions reported by Brace and Nagai (1982) and Matsumura (1995). Generally speaking, when a tooth is relatively small, the surface area per unit volume is rela-

tively large. Since the surface of a developing root is the place where odontoblasts differentiate from the stem cells, a large area per unit volume may represent a large number of odontoblasts per unit volume, leading the rapid PVRrt reduction for Jomon people. Nevertheless, this explanation can not totally explain the present situation, since the sequence of γ was [Jomon < Japanese female < Japanese male], while that of the root volume was [Japanese female < Jomon < Japanese male].

The posterior probabilities of Jomon survival profile

Figure 22 shows the 2-dimensional posterior distributions for the life expectancy at age 15 (e_{15}) and CV of years-to-death after age 15 on gray-scale images. The two prior assumptions are compared in the figure. Not surprisingly, the posterior distribution from the non-uniform prior is on the linear pattern of the human populations, which confirms that the prior distribution properly precluded the unlikely survival patterns as human. On the other hand, the posterior distribution from the uniform priors centers on the ape-like survival pattern, although the distribution is relatively wide and including the human range. While I am not able to deny the possibility of an ape-like survival profile for Jomon people, the disagreement of the uniform priors with the ideal prior distribution might have invoked the shift toward apes. One can imagine on Figure 15 that the uniform distribution on α and β yields high probability density toward the Ⓐ-Ⓑ-Ⓒ side on the log-scale in the lower picture. This yields the high probability density toward the Ⓐ-Ⓑ-Ⓒ side on the e_{15}-CV scale in the upper picture, too (especially toward Ⓐ-Ⓑ side, since the mesh becomes dense toward the side). Therefore, an assumption of the uniform prior means a prior assumption of high probability for monkey-ape survival profiles and low probability for human survival profiles. This assumption disagrees with our empirical knowledge about Jomon people.

Despite all the differences between the results from the both prior assumptions, it can be concluded based on the credible intervals that the life expectancy of Jomon people at age 15 should have been somewhere between 19 and 44 years. When human pattern of survival profile is considered, it should have been between 29 and 42. Compared to the modern hunter-gatherers in Table 5, it is likely that Jomon peo-

ple lived as long as or slightly shorter than they do.

In 1979, Kobayashi argued that the life expectancy at age 15 he had estimated for Jomon people was too short to maintain the population, referring to the model human life tables by Weiss (1973). Weiss (1973) proposed model human life tables sorted by the adult mortality (life expectancy at age 15) and the juvenile mortality (survival rate from age 0 to 15) with the value of gross reproduction rate (GRR[*]) which maintains the population growth ±0. From the data, Kobayashi summarized a table which shows the required GRR to maintain the population according to the population's adult and juvenile mortalities (Table 10). He presumed from data (Henry, 1961) the maximum possible GRR for a human population to be 5.32. And then he recognized that with the life expectancy at age 15 being 15 years or so the population can not be maintained unless unlikely high GRR or hopelessly high juvenile survival rate for the adult mortality is achieved. According to the West level 1 model in Coale and Demeny (1966)—the highest mortality model in their report—the survival rate from age 0 to 15 is about 40% and the life expectancy at age 15 is about 30 years. Assuming the life expectancy to be 30 years for Jomon people upon the result of this study and the juvenile survival rate to be 40% according to the West 1 model, then the required GRR is 3.49 which is fairly achievable number, comparable to the reported number of Yanomama Indians (Neel and Weiss, 1975).

Although the Jomon samples used in this study covered a diverse range of Japanese archipelago and the Jomon period, a great proportion of samples were from the Kanto region and the majority of them were from the Middle–Final Jomon sub-period. Without needing to mention the possibility of genetic diversity in the Jomon population (Adachi et al., 2009), there would have been a variety of life histories over the locations in the archipelago and over the time of Jomon period. Even in the Jomon people sampled in this study, there would have been an amount of heterogeneity about the mortality profiles. I believe, however, that the result of this study does reflect an aspect of the general mortality profiles of "Jomon people." Further investigations encompassing more diverse area and period with detailed analyses will elucidate more

[*] Gross Reproduction Rate is the hypothetical number of daughters that would be born by a female if she experienced the population's age-specific fertility rates through her life to the menopause.

general pattern of Jomon life history, as well as the diversity among them.

Summary

The possible range for the survival profile of Jomon people after age 15 was estimated by Bayesian approaches with uniform and non-uniform prior probabilities. From the results with the uniform priors, the possible range for the life expectancy at age 15 is 19–44 years. Considering the human pattern of survival profile, I suggest that 29–42 years is the most probable range for the expected years of Jomon people at age 15.

References

Aboshi, H., Takahashi, T., & Komuro, T. (2010). Age estimation using microfocus X-ray computed tomography of lower premolars. *Forensic science international*, 200(1), 35-40.

Adachi, N., Shinoda, K. I., Umetsu, K., & Matsumura, H. (2009). Mitochondrial DNA analysis of Jomon skeletons from the Funadomari site, Hokkaido, and its implication for the origins of Native American. *American journal of physical anthropology*, 138(3), 255-265.

Akazawa, T. (1986). Regional variation in procurement systems of Jomon hunter-gatherers. In: Akazawa, T. & Aikens, M. (eds.) *Prehistoric hunter-gatherers in Japan: new research method*, 73-89. Tokyo: University of Tokyo Press.

Andersen, O. (1984). The decline in Danish mortality before 1850 and its economic and social background. In: Bengtsson, T., Fridlizius, G., & Ohlsson, R. (eds.) *Pre-Industrial Population Change*, 115-126. Stockholm: Almquist and Wiksell International.

Arias, E. (2012). United States life tables, 2008. *National vital statistics reports; vol. 58 no. 4*. Hyattsville: National Center for Health Statistics.

Blurton Jones, N. G., Hawkes, K., & O'Connell, J. F. (2002). Antiquity of postreproductive life: Are there modern impacts on hunter-gatherer postreproductive life spans?. *American Journal of Human Biology*, 14(2), 184-205.

Bocquet-Appel, J. P., & Masset, C. (1982). Farewell to paleodemography. *Journal of Human Evolution*, 11(4), 321-333.

Brace, C. L., & Nagai, M. (1982). Japanese tooth size: past and present. *American Journal of Physical Anthropology*, 59(4), 399-411.

Bronikowski, A. M., Alberts, S. C., Altmann, J., Packer, C., Carey, K. D., & Tatar, M. (2002). The aging baboon: comparative demography in a non-human primate. *Proceedings of the National Academy of Sciences*, 99(14), 9591-9595.

Caussinus, H., & Courgeau, D. (2010). Estimating age without measuring it: A new method in paleodemography. *Population (english edition)*, 65(1), 117-144.

Coale, A. J. & Demeny, P. (1966). *Regional model life tables and stable populations.* Princeton: Princeton Univ. Press.

Di Bacco, M., Ardito, V., & Pacciani, E. (1999). Age-at-death diagnosis and age-at-death distribution estimate: Two different problems with many aspects in common. *International Journal of Anthropology*, 14(2), 161-169.

Dyke, B., Gage, T. B., Mamelka, P. M., Goy, R. W., & Stone, W. H. (1986). A demographic analysis of the Wisconsin Regional Primate Center rhesus colony, 1962–1982. *American Journal of Primatology*, 10(3), 257-269.

Dyke, B., Gage, T. B., Alford, P. L., Swenson, B., & Williams-Blangero, S. (1995). Model life table for captive chimpanzees. *American Journal of Primatology*, 37(1), 25-37.

Fedigan, L. M., & Zohar, S. (1997). Sex differences in mortality of Japanese macaques: twenty-one years

of data from the Arashiyama West population. *American journal of physical anthropology*, 102(2), 161-175.

Gustafson, G. (1950). Age estimation on teeth. *Journal of the American Dental Association*, 41, 435-54.

Ha, J. C., Robinette, R. L., & Sackett, G. P. (2000). Demographic analysis of the Washington Regional Primate Research Center pigtailed macaque colony, 1967-1996. *American journal of primatology*, 52(4), 187-198.

Habu, J. (2004). *Ancient Jomon of Japan*. Cambridge: Cambridge University Press.

Hanihara, K. (1991). Dual structure model for the population history of the Japanese. *Nichibunken Japan Review*, 1-33.

Henry, L. (1961). Some data on natural fertility. *Eugenics Quarterly*, 8, 81-91.

Herrmann, N. P., & Konigsberg, L. W. (2002). A re-examination of the age-at-death distribution of Indian Knoll. In: Hoppa, R. D. & Vaupel J. W. (eds.) *Paleodemography: age distributions from skeletal samples*, 243-257. Cambridge: Cambridge University Press.

Hill, K. R., & Hurtado, A. M. (1996). *Ache life history: The ecology and demography of a foraging people*. New York: Walter de Gruyter.

Hill, K., Boesch, C., Goodall, J., Pusey, A., Williams, J., & Wrangham, R. (2001). Mortality rates among wild chimpanzees. *Journal of Human Evolution*, 40(5), 437-450.

Holman, D. J., Wood, J. W., & O Connor, K. A. (2002). Estimating age-at-death distributions from skeletal samples: a multivariate latent-trait approach. In: Hoppa, R. D. & Vaupel J. W. (eds.) *Paleodemography: age distributions from skeletal samples*, 193-221. Cambridge: Cambridge University Press.

Hoppa, R. D., & Vaupel, J. W. (2002). The Rostock Manifesto for paleodemography: The way from stage to age. In: Hoppa, R. D. & Vaupel J. W. (eds.) *Paleodemography: age distributions from skeletal samples*, 1-8. Cambridge: Cambridge University Press.

Howell, N. (1979). *Demography of the Dobe !Kung*. New York: Academic Press.

Jannetta, A. B., & Preston, S. H. (1991). Two centuries of mortality change in central Japan: the evidence from a temple death register. *Population Studies*, 45(3), 417-436.

Keally, C. T., & Muto, Y. (1982). Jomon jidai no nendai [Dating of the Jomon period]. In: Kato, S., Kobayashi, T., & Fujimoto, T. (eds.) *Jomon bunka no kenkyu I, Jomon-jin to sono Kankyo [Studies of the Jomon Culture, vol. 1, The Jomon People and the Surrounding Environment]*, 246-275. Tokyo: Yuzankaku (in Japanese).

Kikuchi, M. (1983). Kamekan-so [Jar burials]. In: Kato, S., Kobayashi, T., & Fujimoto, T. (eds.) *Jomon bunka no kenkyu IX, Jomon-jin no seishin bunka [Studies of the Jomon culture, vol. IX, mortuary and ceremonial practices]*, 57-71. Tokyo: Yuzankaku (in Japanese).

Kobayashi, K. (1964). Estimation of age at death from pubic symphysis for the prehistoric human skeletons in Japan. *Jinruigaku zasshi*, 72(2), 43-55 (in Japanese).

Kobayashi, K. (1967). Trend in the length of life based on human skeletons from prehistoric to modern times in Japan. *Journal of Faculty of Science, the University of Tokyo, Section V*, 3, 107-162.

Kobayashi, K. (1979). Jinkou-Jinruigaku [Paleodemography]. In: Kobayashi, K. (ed.) *Jinruigaku Kouza 11: Jinkou [Anthropology 11: Demography]*, 63-129. Tokyo: Yuzankaku (in Japanese).

Konigsberg, L. W., & Frankenberg, S. R. (2002). Deconstructing death in paleodemography. *American Journal of Physical Anthropology*, 117(4), 297-309.

Konigsberg, L. W., & Herrmann, N. P. (2002). Markov chain Monte Carlo estimation of hazard model parameters in paleodemography. In: Hoppa, R. D. & Vaupel J. W. (eds.) *Paleodemography: age distributions from skeletal samples*, 222-242. Cambridge: Cambridge University Press.

Kusaka, S., Hyodo, F., Yumoto, T., & Nakatsukasa, M. (2010). Carbon and nitrogen stable isotope analysis on the diet of Jomon populations from two coastal regions of Japan. *Journal of Archaeological Science*, 37(8), 1968-1977.

Kvaal, S., & Solheim, T. (1994). A non-destructive dental method for age estimation. *The Journal of forensic odonto-stomatology*, 12(1), 6-11.

Lancaster, H. O. (1959). Generation life tables for Australia. *Australian Journal of Statistics*, *1*(1), 19-33.

Langley - Shirley, N., & Jantz, R. L. (2010). A Bayesian Approach to Age Estimation in Modern Americans from the Clavicle. *Journal of forensic sciences*, 55(3), 571-583.

Lee, R. (1984). Mortality levels and agrarian reforms in early 19th century Prussia: some regional evidence. In: Bengtsson, T., Fridlizius, G., & Ohlsson, R. (eds.) *Pre-Industrial Population Change*, 161-190. Stockholm: Almquist and Wiksell International.

Matsumura, H. (1995). A microevolutional history of the Japanese people as viewed from dental morphology. *National Science Museum Monographs*, 9, 1-130.

Masui, K., Sugiyama, Y., Nishimura, A., & Ohsawa, H. (1974). The life table of Japanese monkeys at Takasakiyama: a preliminary report. In: Kondo, S., Kawai, M., & Ehara, A. (eds.) *Contemporary Primatology 5th Int. Congr. Primat., Nagoya 1974*, 401-406. Basel: Karger.

Matsui, A., & Kanehara, M. (2006). The question of prehistoric plant husbandry during the Jomon period in Japan. *World Archaeology*, 38(2), 259-273.

McKern, T. W., & Stewart, T. D. (1957). *Skeletal age changes in young American males*. Natick, MA: Headquarters Quartermaster Research and Development Command.

Minagawa, M., & Akazawa, T. (1992). Dietary patterns of Japanese Jomon hunter-gatherers: Stable nitrogen and carbon isotope analyses of human bones. In: Aikens, C. M. & Rhee, S. N. (eds.) *Pacific Northeast Asia in Prehistory:Hunter-Fisher-Gatherers, Farmers, and Sociopolitical Elites*, 59-68. Pullman: Washington State University Press.

Ministry of Health, Labour and Welfare (2012). Dai21kai seimeihyou (kannzen-seimeihyou) no gaikyou [The 21st life table (based on the national census)]. Retrieved December 5, 2013 from website < http://www.mhlw.go.jp/toukei/saikin/hw/life/21th/index.html> (in Japanese).

Ministry of Health, Labour and Welfare (undated). Heisei17-nen shika-shikkan jittai-chousa [Dental survey as of 2005]. Retrieved November 1, 2013 from website <http://www.mhlw.go.jp/toukei/list/62-17c.html> (in Japanese).

Moorrees, C. F., Fanning, E. A., & Hunt, E. E. (1963). Age variation of formation stages for ten permanent teeth. *Journal of dental research*, 42(6), 1490-1502.

Nagaoka, T., Sawada, J., & Hirata, K. (2008). Did the Jomon people have a short lifespan? Evidence from the adult age-at-death estimation based on the auricular surface of the ilium. *Anthropological Science*,

116(2), 161-169.

Naito, Y. I., Chikaraishi, Y., Ohkouchi, N., & Yoneda, M. (2013). Evaluation of carnivory in inland Jomon hunter-gatherers based on nitrogen isotopic compositions of individual amino acids in bone collagen. *Journal of Archaeological Science* 40, 2913-2923.

Nakamura, T., Taniguchi, Y., Tsuji, S., & Oda, H. (2001). Radiocarbon dating of charred residues on the earliest pottery in Japan. *Radiocarbon*, 43(2B), 1129-1138.

Neel, J. V. & Weiss, K. M. (1975). The genetic structure of a tribal population, the Yanomama Indians. *American journal of physical anthropology*, 42(1), 25-51.

Office for National Statistics (2013). Statistical Bulletin—Interim life tables, England and Wales, 2010–2012. Newport: Office for National Statistics.

Perrenoud, A. (1984). The mortality decline in a long-term perspective. In: Bengtsson, T., Fridlizius, G., & Ohlsson, R. (eds.) *Pre-Industrial Population Change*, 41-69. Stockholm: Almquist and Wiksell International.

Preston, S. H., Keyfitz, N., & Schoen, R. (1972). *Causes of Death: Life Tables for National Population.* New York: Seminar Press.

Sade, D. S., Cushing, K., Cushing, P., Dunaif, J., Figueroa, A., Kaplan, J. R., Lauer, C., Rhodes, D., & Schneider, J. (1976). Population dynamics in relation to social structure on Cayo Santiago. *Yearbook of Physical Anthropology*, 20, 253-262.

Séguy, I., Caussinus, H., Courgeau, D., & Buchet, L. (2013). Estimating the age structure of a buried adult population: A new statistical approach applied to archaeological digs in France. *American journal of physical anthropology*, 150(2), 170-183.

Someda, H., Saka, H., Matsunaga, S., Ide, Y., Nakahara, K., Hirata, S., & Hashimoto, M. (2009). Age estimation based on three-dimensional measurement of mandibular central incisors in Japanese. *Forensic science international*, 185(1), 110-114.

Spoor, C. F., Zonneveld, F. W., & Macho, G. A. (1993). Linear measurements of cortical bone and dental enamel by computed tomography: applications and problems. *American Journal of Physical Anthropology*, 91(4), 469-484.

Star, H., Thevissen, P., Jacobs, R., Fieuws, S., Solheim, T., & Willems, G. (2011). Human Dental Age Estimation by Calculation of Pulp–Tooth Volume Ratios Yielded on Clinically Acquired Cone Beam Computed Tomography Images of Monoradicular Teeth. *Journal of Forensic Sciences*, 56(s1), S77-S82.

Statistics Canada (2013). Life tables, Canada, provinces and territories, 2009 to 2011. Ottawa: Statistics Canada.

Storey, R. (2007). An elusive paleodemography? A comparison of two methods for estimating the adult age distribution of deaths at late Classic Copan, Honduras. *American journal of physical anthropology*, 132(1), 40-47.

Tigges, J., Gordon, T. P., McClure, H. M., Hall, E. C., & Peters, A. (1988). Survival rate and life span of rhesus monkeys at the Yerkes Regional Primate Research Center. *American Journal of Primatology*, 15(3), 263-273.

United Nations (1986). *Age structure of mortality in developing countries: a data base for cross-sectional and time series research*. New York: United Nations.

Vandevoort, F. M., Bergmans, L., Van Cleynenbreugel, J., Bielen, D. J., Lambrechts, P., Wevers, M., Peris, A. & Willems, G. (2004). Age calculation using X-ray microfocus computed tomographical scanning of teeth: a pilot study. *Journal of forensic sciences*, 49(4), 787-790.

Walker, P. L., Johnson, J. R., & Lambert, P. M. (1988). Age and sex biases in the preservation of human skeletal remains. *American Journal of Physical Anthropology*, 76(2), 183-188.

WHO (2013a). Life tables, Global Health Observatory Data Repository. Retrieved December 5, 2013 from website < http://apps.who.int/gho/data/node.main.692?lang=en>.

WHO (2013b). *WHO methods and data sources for life tables 1990–2011*. Geneva: WHO. available at < http://www.who.int/healthinfo/statistics/mortality/en/index3.html>.

Wich, S. A., Utami-Atmoko, S. S., Setia, T. M., Rijksen, H. D., Schürmann, C., Van Hooff, J. A. R. A. M., & van Schaik, C. P. (2004). Life history of wild Sumatran orangutans (*Pongo abelii*). *Journal of Human Evolution*, 47(6), 385-398.

Wood, J. W., Holman, D. J., O Connor, K. A., & Ferrell, R. J. (2002). Mortality models for paleodemography. In: Hoppa, R. D. & Vaupel J. W. (eds.) *Paleodemography: age distributions from skeletal samples*, 129-168. Cambridge: Cambridge University Press.

Wrigley, E. A., Davis, R. S., Oeppen, J. E. & Schofield, R. S. (1997). *English population history from family reconstitution 1580-1837*. Cambridge: Cambridge University Press.

Yang, F., Jacobs, R., & Willems, G. (2006). Dental age estimation through volume matching of teeth imaged by cone-beam CT. *Forensic science international*, 159, S78-S83.

Table 1. Age and sex distribution of reference samples (recent-modern Japanese).

Age category [yrs]	Male	Female	Total
15–19	18	3	21
20–29	33	29	62
30–39	33	16	49
40–49	32	23	55
50–59	31	22	53
60–69	30	28	58
≥70	32	33	65
Total	209	154	363

Table 2. Means of [1]PVRrt for each sex and age-class, and the results of *t* -tests among them (Japanese samples).

	15–19		20–29		30–39		40–49		50–59		60–69		≥70
Male mean (in %) and inter-age class comp.	7.10	**	5.67	**	4.61	NS (0.63)	4.48	**	3.83	NS (0.98)	3.82	NS (0.59)	3.96
inter-sex comparison	NS (0.95)		NS (0.43)		NS (0.76)		**		NS (0.31)		**		**
Female mean (in %) and inter-age class comp.	7.06	*	5.47	**	4.50	*	3.62	NS (0.84)	3.55	*	2.94	NS (0.07)	2.57

[1]Pulp Volume Ratio within a root portion of lower-canine.
() show the *P* values when the tests resulted Not Significant with significance level of 0.05.
*,*P* <0.05; **,*P* <0.01. See Table 1 for the numbers of the samples.

Table 3. Parameters of the PVRrt reduction model determined for recent-modern Japanese.

	A	γ	D	S
Male	-5.17×10^{-2}	3.49×10^{-2}	7.36×10^{-2}	1.085×10^{-2}
Female	-5.17×10^{-2}	2.58×10^{-2}	7.36×10^{-2}	0.904×10^{-2}

A: shape factor of the curve (shared by male&female), γ: asymptotic line,
D: initial value at age 15 (shared by male&female), S: σ of the normal distribution

Table 4. Parameters estimated by the maximum likelihood approach for Jomon people.

	α	β	γ	λ	θ
Result	3.751×10^{-3}	5.465×10^{-2}	1.915×10^{-2}	3.195×10^{-1}	-2.904×10^{-3}

(α,β): parameters of the Gompertz model, γ: asymptotic line of PVRrt reduction,
λ: probability at age 15 of retaining a clavicle conditional on retaining a lower canine,
θ: slope of the probability change with age

Table 5. The populations used to calculate the non-uniform prior distribution.

	location/identification	observation period	e_{15}	CV	note	source
Current human population	39 countries[*1]	2011	—	—		WHO, 2013a
	Canada	2009–2011	67.22	0.192		Statistics Canada, 2013
	England and Wales	2010–2012	66.61	0.185		ONS, 2013
	Japan	2010	68.58	0.180		MHLW, 2012
	USA	2008	64.28	0.220		Arias, 2012
Historical human population	30 developing countries[*2]	1945–1978	—	—		United Nations, 1986
	48 countries[*3]	1861–1964	—	—		Preston et al., 1972
	Denmark	1790–1794	44.82	0.452		Andersen, 1984
	Hida, Japan	1776–1795	44.47	0.422		Jannetta & Preston, 1991
	Australia	1881–1885	46.99	0.446		Lancaster, 1959
	Oldenburg, Germany	1855–1864	42.11	0.439		Lee, 1984
	Geneva	1625–1649	36.35	0.513		Perrenoud, 1984
	England	1640–1689	37.73	0.502		Wrigley et al., 1997
Modern hunter-gatherer	Ache	The forest period (before 1971)	39.78	0.520		Hill & Hurtado, 1996
	!Kung	1964–1973	54.90	0.262		Howell, 1979
	Hadza	1985–1990	44.47	0.453		Blurton Jones et al., 2002
Orangutan (*Pongo abelii)*	Katambe	1971–2003	27.73	0.430	Wild	Wich et al., 2004
Chimpanzee (*Pan troglodytes*)	3 breeding colonies combined	—	22.99	0.541	Captive	Dyke et al., 1995
	Gombe	1963–1998	16.02	0.467	Wild	Hill et al., 2001
	Taï	1982–1994	9.34	0.815	Wild	Hill et al., 2001
	Kibale	1987–1998	26.72	0.423	Wild	Hill et al., 2001
Baboon (*Papio hamadryas*)	Amboseli	1971–1999	7.14	0.556	Wild	Bronikowski, 2002
	Gombe	1968–2000	10.71	0.443	Wild	Bronikowski, 2002
	Southwest Foundation for Biomedical Research	1964–2000	11.67	0.491	Captive	Bronikowski, 2002
Rhesus monkey (*Macaca mulatta*)	Wisconsin Regional Primate Center	1962–1982	14.07	0.656	Captive	Dyke et al., 1986
	Cayo, Santiago	1973–1974	4.41	0.764	Provisioned	Sade et al., 1976
	Yerkes Regional Primate Research Center	1969–1987	6.14	0.669	Captive	Tigges et al., 1988 (sample group II)
Japanese monkey (*Macaca fuscata*)	A ranch in Texas	1972–1993	8.38	0.573	Provisioned	Fedigan & Zohar, 1997
	Takasakiyama, Japan	1962–1970	5.62	0.809	Provisioned	Masui et al., 1975
Pigtailed macaque (*Macaca nemestrina*)	The University of Washington's Regional Primate Research Center	1967–1996	5.95	0.717	Captive	Ha et al., 2000

e_{15} and CV were calculated by fitting the Gompertz model to the reported data, except for Baboon where the Gompertz parameters they reported were directly used. See Appendix A for the fitting methods.
Only female data were used for all cercopithecine monkeys.

[*1]Those countries whose data completeness was categorized as "A" were selected for this study (WHO, 2013b).

[*2]Those life tables of countries and periods which did not overlap with the other sources were selected.

[*3]When multiple periods were avilable for a country the oldest life table was selected.

Table 6. The sample variance-covariance matrix.

	e_{15}	CV
e_{15}	45.13	-0.5381
CV	-0.5381	7.485×10^{-3}

df=N-2=128, M_e=54.32, M_{cv}=0.3078.

The parameters in equation (4.3)

(See, Sec, V) can be derived from the matrix.

Table 7. Means and 95% credible intervals by the Bayesian approach with uniform priors.

	2.5 percentile value	mean (median)	97.5 percentile value
α	0.885×10^{-3}	$3.897(3.551) \times 10^{-3}$	8.700×10^{-3}
β	2.361×10^{-2}	$6.392(5.988) \times 10^{-2}$	12.534×10^{-2}
γ	0.734×10^{-2}	$1.730(1.793) \times 10^{-2}$	2.422×10^{-2}
λ	1.553×10^{-1}	$3.176(3.150) \times 10^{-1}$	4.987×10^{-1}
θ	-9.254×10^{-3}	$-2.823(2.743) \times 10^{-3}$	3.111×10^{-3}
e_{15}[yrs]	19.45	29.50(28.65)	43.60

(α,β): parameters of the Gompertz model, γ: the asymptotic line of PVRrt reduction,
λ: probability at age 15 of retaining a clavicle conditional on retaining a lower canine,
θ: slope of the probability change with age, e_{15}: life expectancy at age 15

Table 8. Means and 95% credible intervals by the Bayesian approach with non-uniform prior for α and β.

	2.5 percentile value	mean (median)	97.5 percentile value
α	2.767×10^{-3}	$5.130(4.962) \times 10^{-3}$	8.475×10^{-3}
β	3.062×10^{-2}	$4.031(4.004) \times 10^{-2}$	5.136×10^{-2}
γ	1.710×10^{-2}	$2.107(2.117) \times 10^{-2}$	2.453×10^{-2}
λ	1.758×10^{-1}	$3.284(3.241) \times 10^{-1}$	5.013×10^{-1}
θ	-7.318×10^{-3}	$-2.680(2.610) \times 10^{-3}$	1.608×10^{-3}
e_{15}[yrs]	29.19	35.19(35.13)	41.52

(α,β): parameters of the Gompertz model, γ: the asymptotic line of PVRrt reduction, λ: probability at age 15 of retaining a clavicle conditional on retaining a lower canine, θ: slope of the probability change with age, e_{15}: life expectancy at age 15

Table 9. The mode value of the posterior distribution from the Bayesian approach with non-uniform prior for α and β.

	α	β	γ	λ	θ
Result	4.821×10^{-3}	3.952×10^{-2}	2.153×10^{-2}	3.109×10^{-1}	-2.250×10^{-3}

(α,β): parameters of the Gompertz model, γ: asymptotic line of PVRrt reduction,
λ: probability at age 15 of retaining a clavicle conditional on retaining a lower canine,
θ: slope of the probability change with age

Table 10. The Gross Reproduction Rate (GRR) required to maintain the population, derived from the model life tables by Weiss (1973).

Survival rate from age 0 to 15. (%)	Life expectancy at age 15 (yrs)							
	15.0	20.0	22.5	25.0	27.5	30.0	32.5	35.0
30	7.16	5.84	5.44	5.12	4.86	4.65	4.47	4.31
35	6.13	5.01	4.66	4.39	4.17	3.98	3.83	3.69
40	5.37	4.38	4.08	3.84	3.65	3.49	3.35	3.23
45	4.77	3.90	3.62	3.41	3.24	3.10	2.98	2.87
50	4.29	3.51	3.26	3.07	2.92	2.79	2.68	2.58
55	3.90	3.19	2.97	2.79	2.65	2.54	2.44	2.35
60	3.58	2.92	2.72	2.56	2.43	2.32	2.23	2.15
65	3.30	2.70	2.51	2.36	2.24	2.15	2.06	1.99
70	3.07	2.50	2.33	2.19	2.08	1.99	1.91	1.85

This table was made by Kobayashi (1979) by collecting the data from the model lefe tables in Weiss (1973).
The solid line is the maxmum possible GRR=5.3 for human populations presumed by Kobayashi (1979) from the data by Henry (1961).
The doted line is GRR=3.9 for Yanomama Indians calculated by Kobayashi (1979) from the data reported by Neel & Weiss (1975).

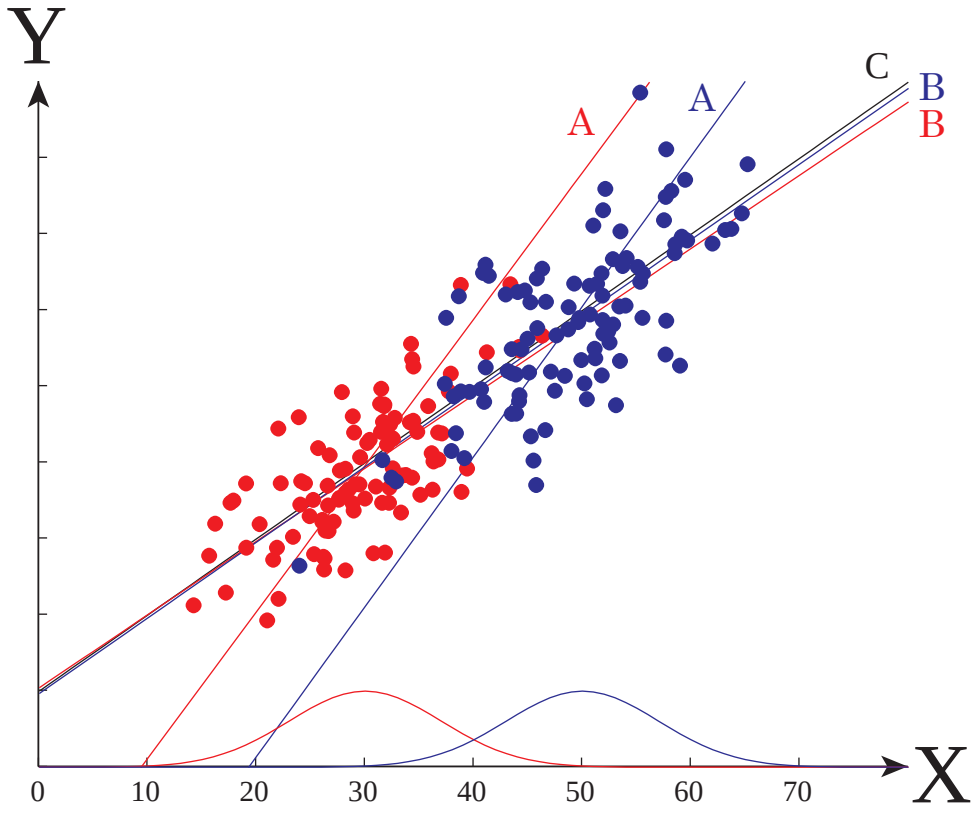

Figure 1. Results of inverse regression from different distributions of the independent variable (X). The plots were generated computationally so that Y is determined by X according to a linear function (C) with a normal distribution of error. X were generated so as to distribute normal, but with smaller mean for red plots and larger mean for blue plots. The set of (A) indicates the results of linear regression of X on Y. The set of (B) indicates the results of linear regression of Y on X. The former results classified as inverse regressions differ between the groups, while the latter classified as forward regressions are nearly identical.

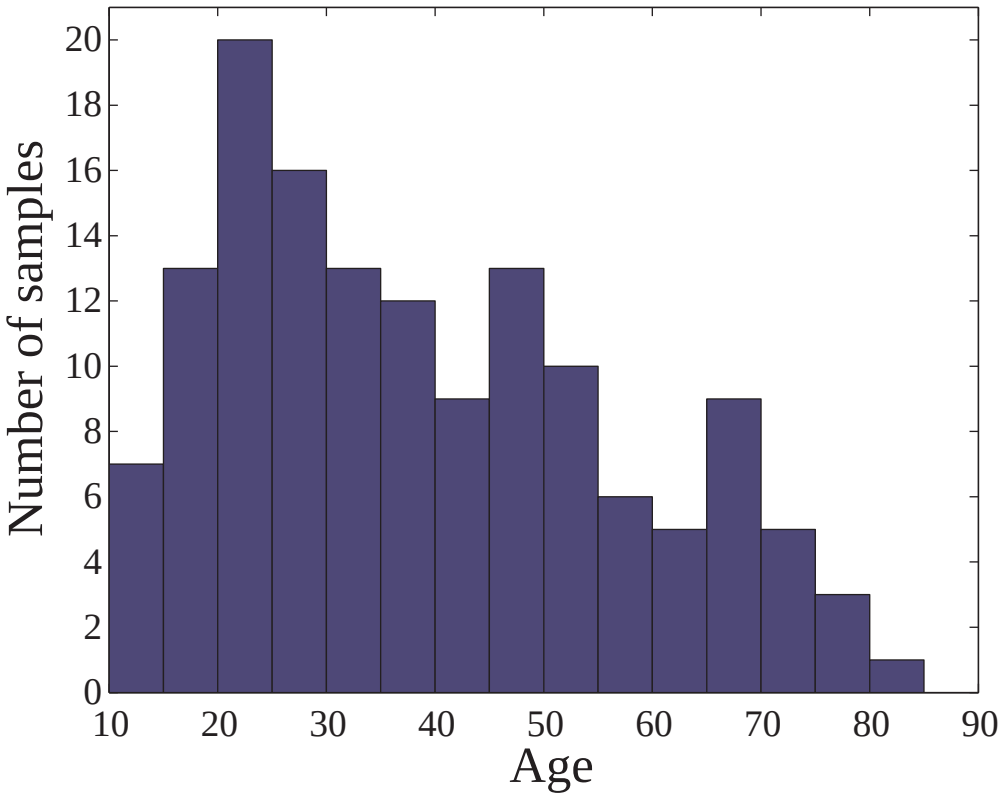

Figure 2. Age distribution of the reference skeletons which were used in Kobayashi (1967). Redrawn from Kobayashi, 1967, Table 1.

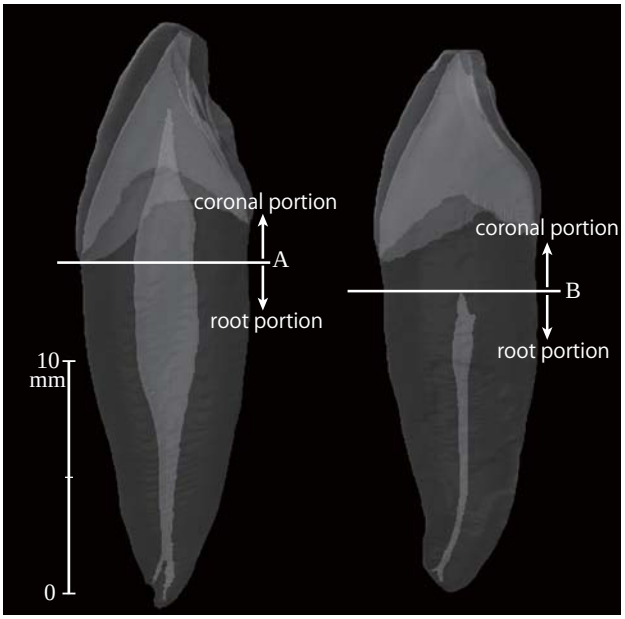

Figure 3. Semi-transparent imageries of lower canine teeth in lateral view. Left: 26-year-old female. Right: 53-year-old male. The flat horizontal plane that bisects the teeth into coronal and root portions was defined as that at the height of apical-most point of cementoenamel junction, or at the height of coronal-most point of pulp cavity, whichever was more apical. (A) exemplifies the former case, (B) exemplifies the latter. Only root portions were considered for the analyses in this study.

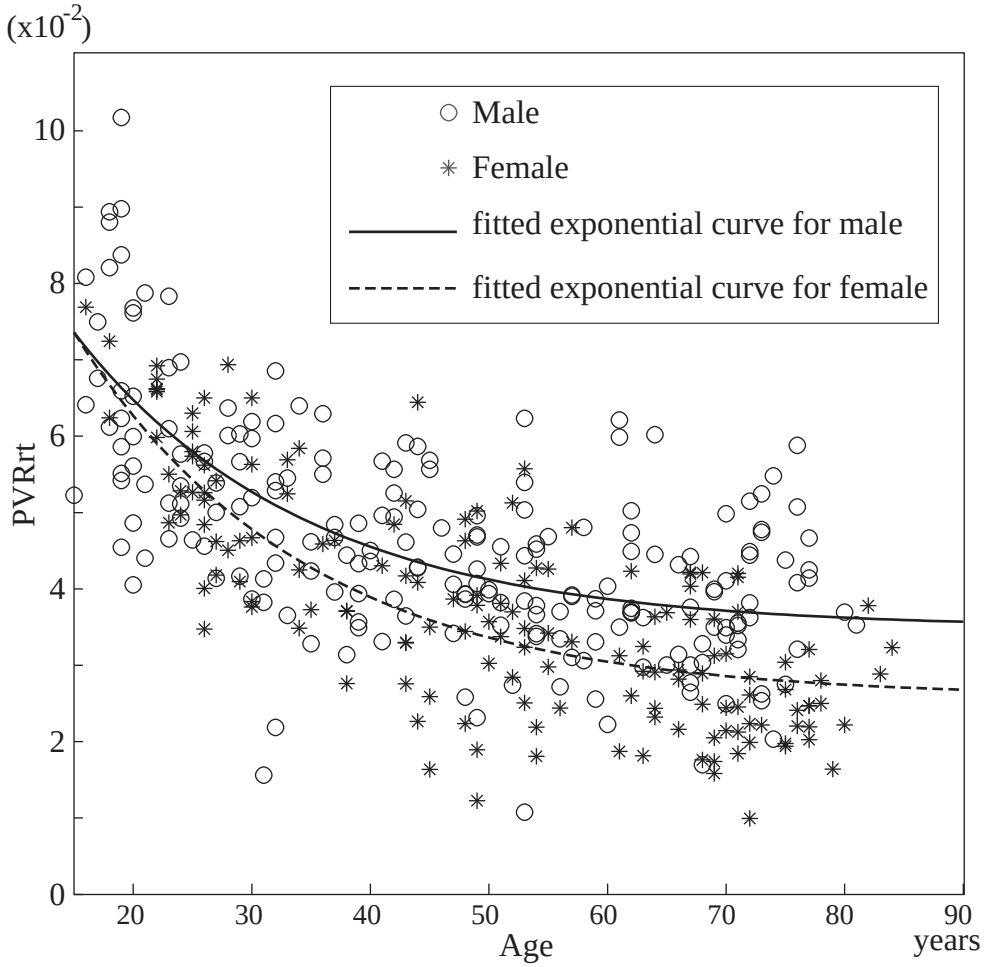

Figure 4. The PVRrt (pulp volume ratio in root) reduction with age observed in 363 recent-modern Japanese lower canines. Exponential model was fitted to the data by the maximum likelihood method. See text in Chapter II for the detail of the model.

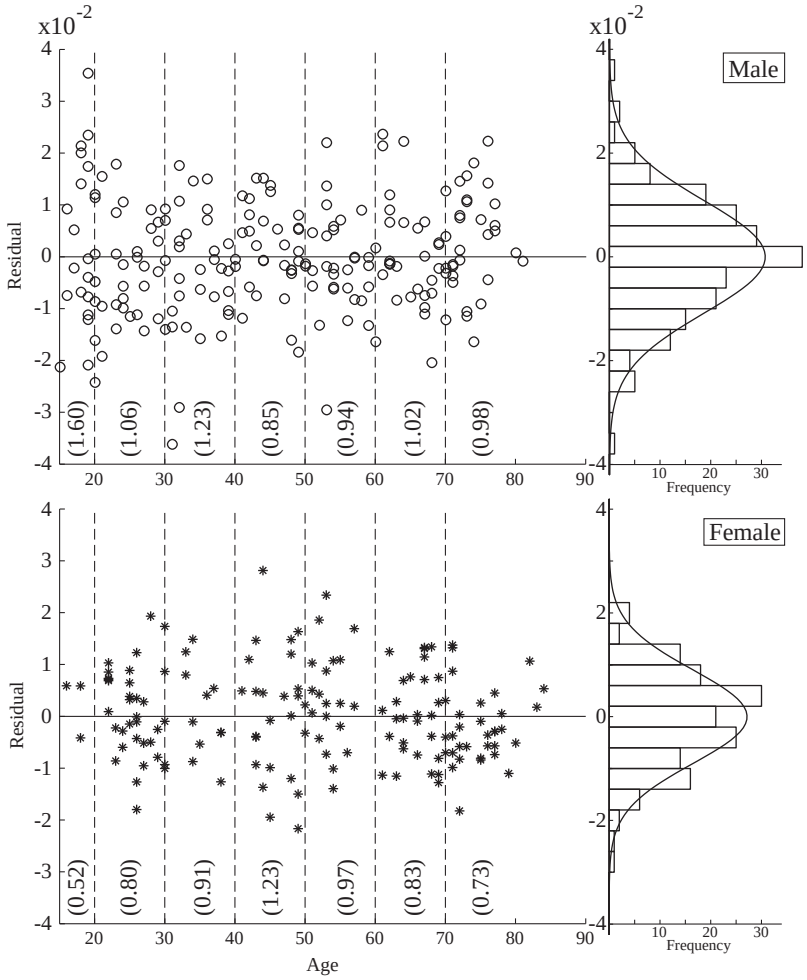

Figure 5. Scatter diagrams of residuals and their histograms, for males and females. Residuals are signed distances of PVRrt observations from the fitted exponential curves (see Figure 4). The curves on the histograms are the normal distribution of mean = 0, s.d. = sample s.d. The parentheses indicate deviation of the residuals in each age-category calculated as $\sqrt{\frac{1}{n}\sum(residual)^2}$.

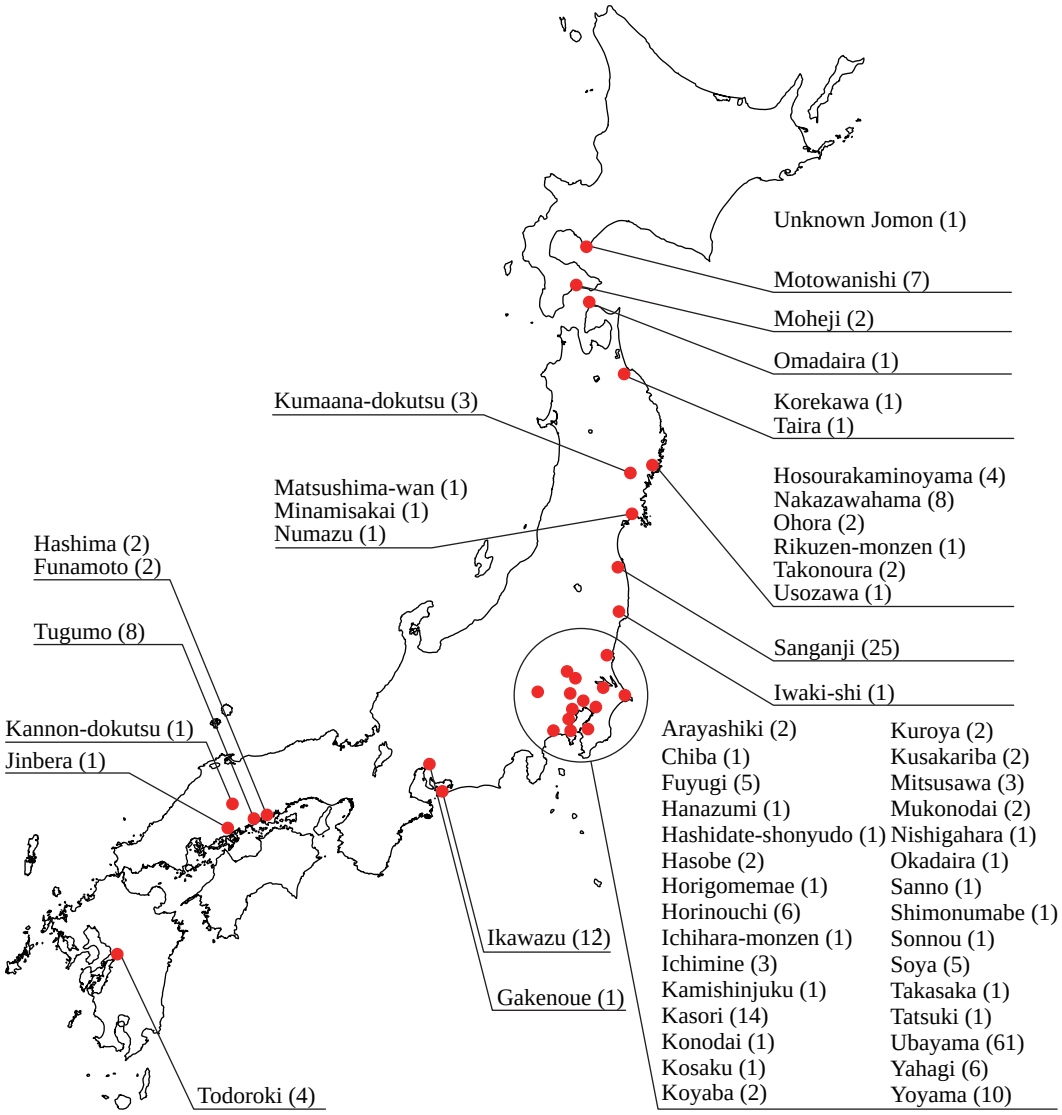

Figure 6. Locations of the sites where the skeletal samples used in this study had been excavated. Parentheses indicate the number of individuals (those from whom the lower canines were collected).

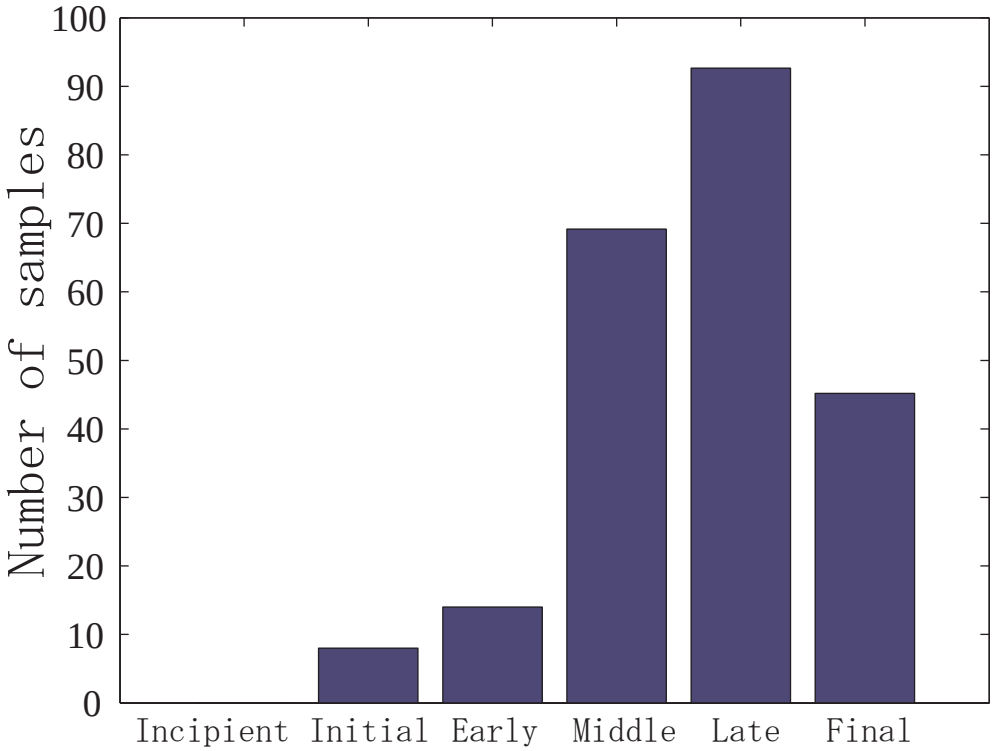

Figure 7. The sample distribution according to the Jomon sub-periods. Incipient, Initial, Early, Middle, Late, and Final sub-periods are corresponding to ca. 13000–9500, 9500–6000, 6000–5000, 5000–4000, 4000–3000, and 3000–2300 years BP, respectively. The number of individuals whose site had ranged across multiple sub-periods were divided by the number of sub-periods and allocated to each of them.

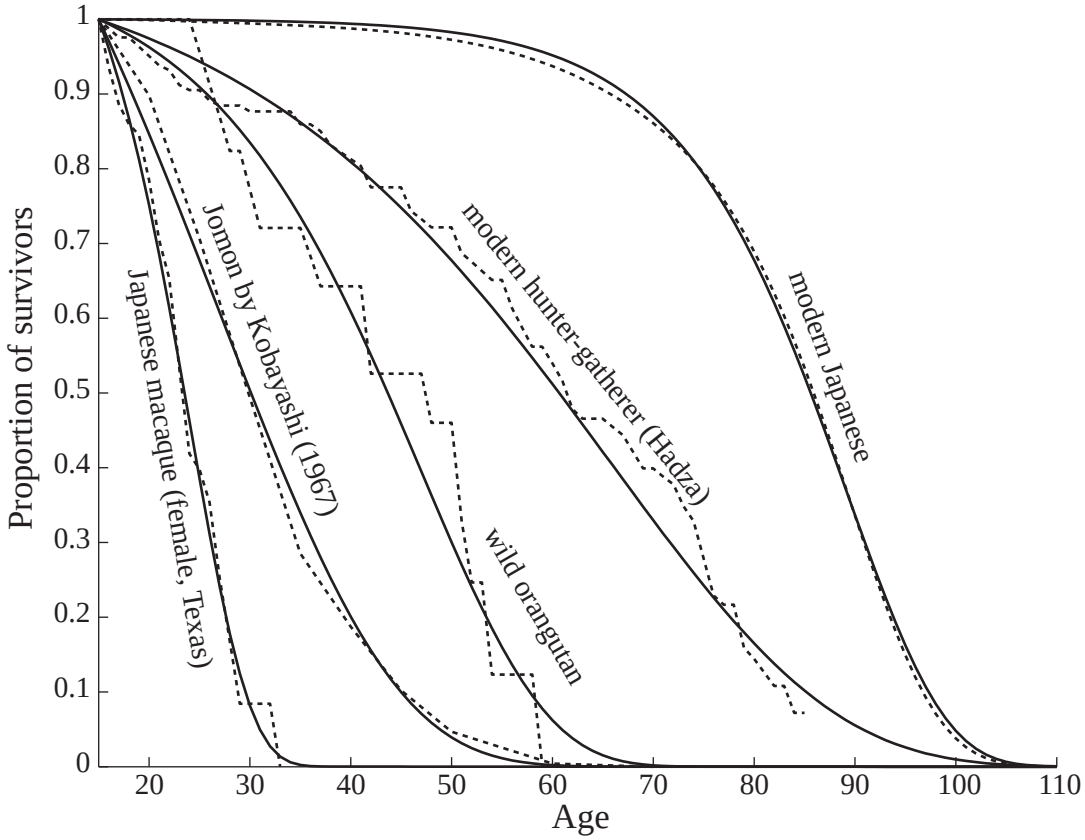

Figure 8. Fitted Gompertz models to several survival lines. Dotted line indicates the survival line (lx) according to the reported life tables. Male and female data were combined, except for Japanese macaque. Solid line indicates the survival curve of the Gompertz model fitted to the data by the least square or maximum likelihood methods. See Appendix A for the details of the fitting method. See Table 5 for the data sources.

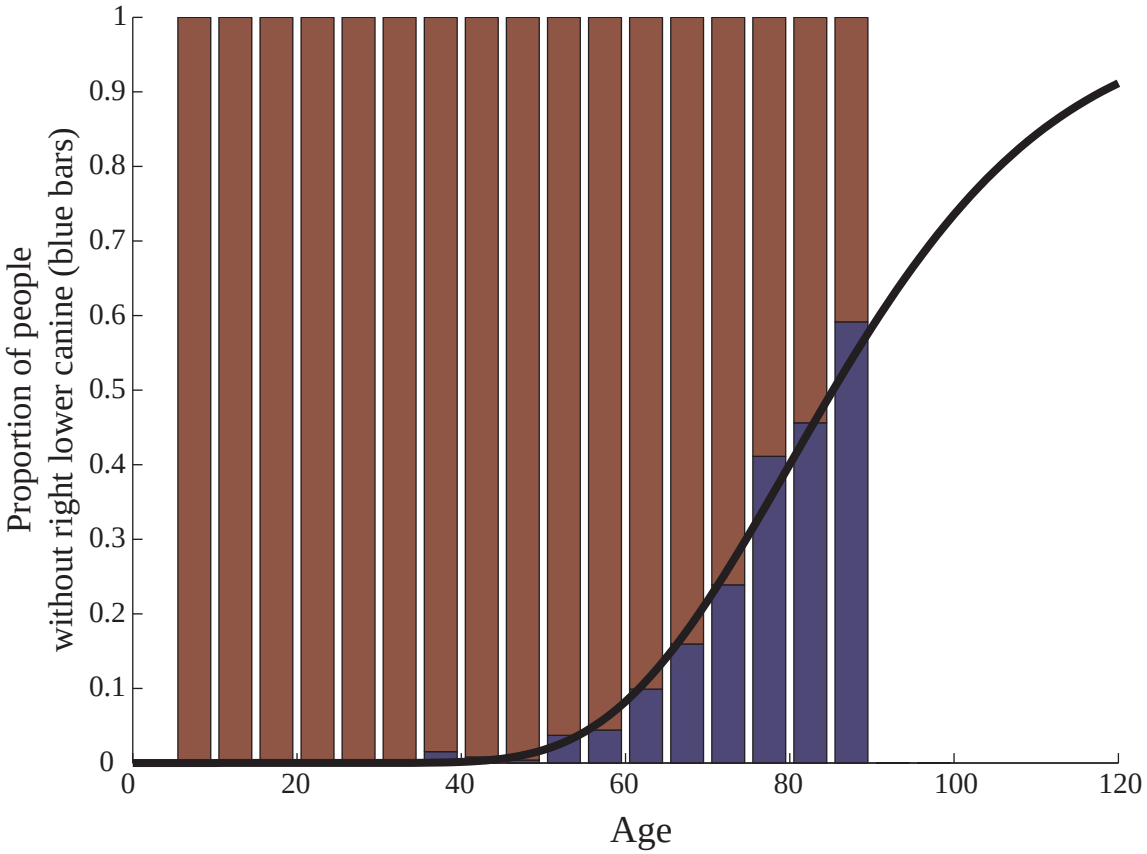

Figure 9. The rate of right lower canine loss increaseing with age and the fitted log-probit model. Data are of Japanese as of 2005 reported by Ministry of Health, Labour, and Welfare (undated).

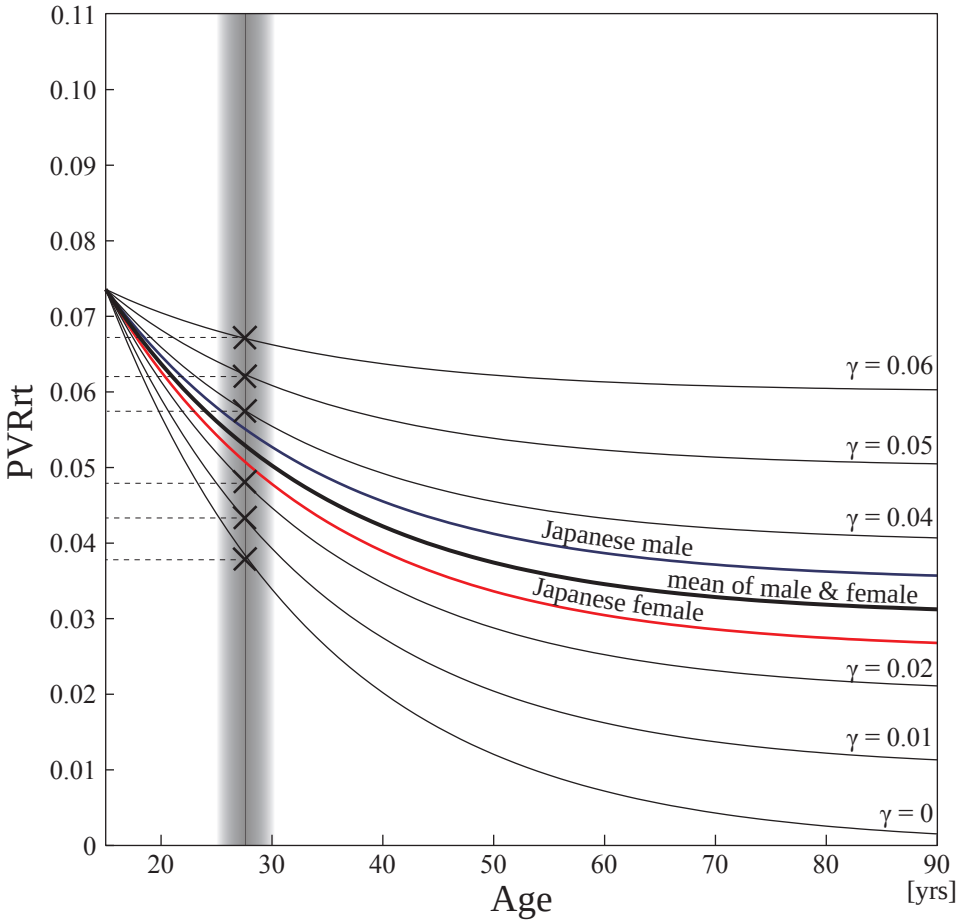

Figure 10. The PVRrt exponential curves varying according to γ. PVRrt=γ is asymptote of the exponential curve. The gray gradation indicates the late 20s of age, the general time for the sternal epiphysis closure of the clavicle. Clavicle observations on Jomon samples restrain the possible range of γ, since the exponential curve should pass the general area of intersection between the gray band and the PVRrt value corresponding to the occurrence of the closure.

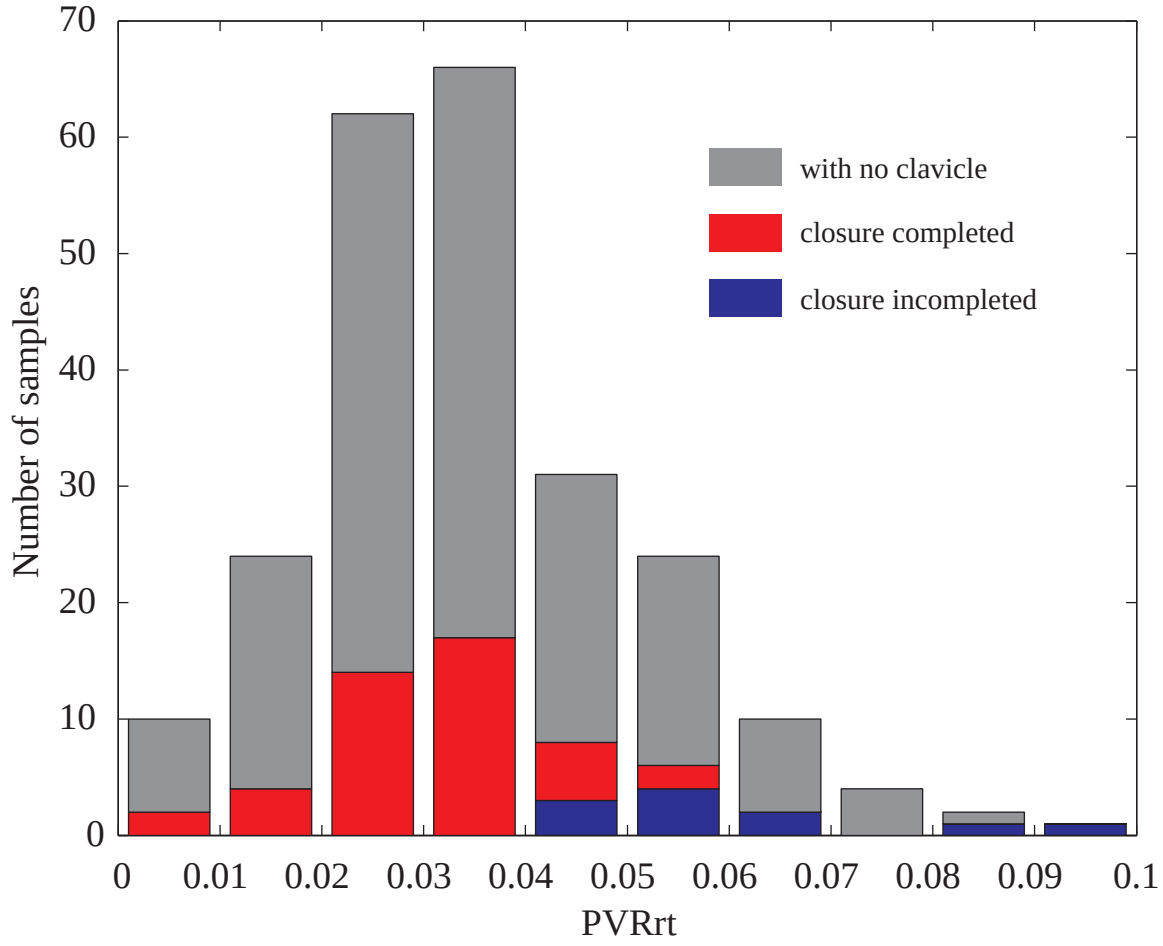

Figure 11. The distribution of PVRrt and the states of epiphyseal closure and preservation at sternal end of the clavicle observed in the 234 Jomon individuals.

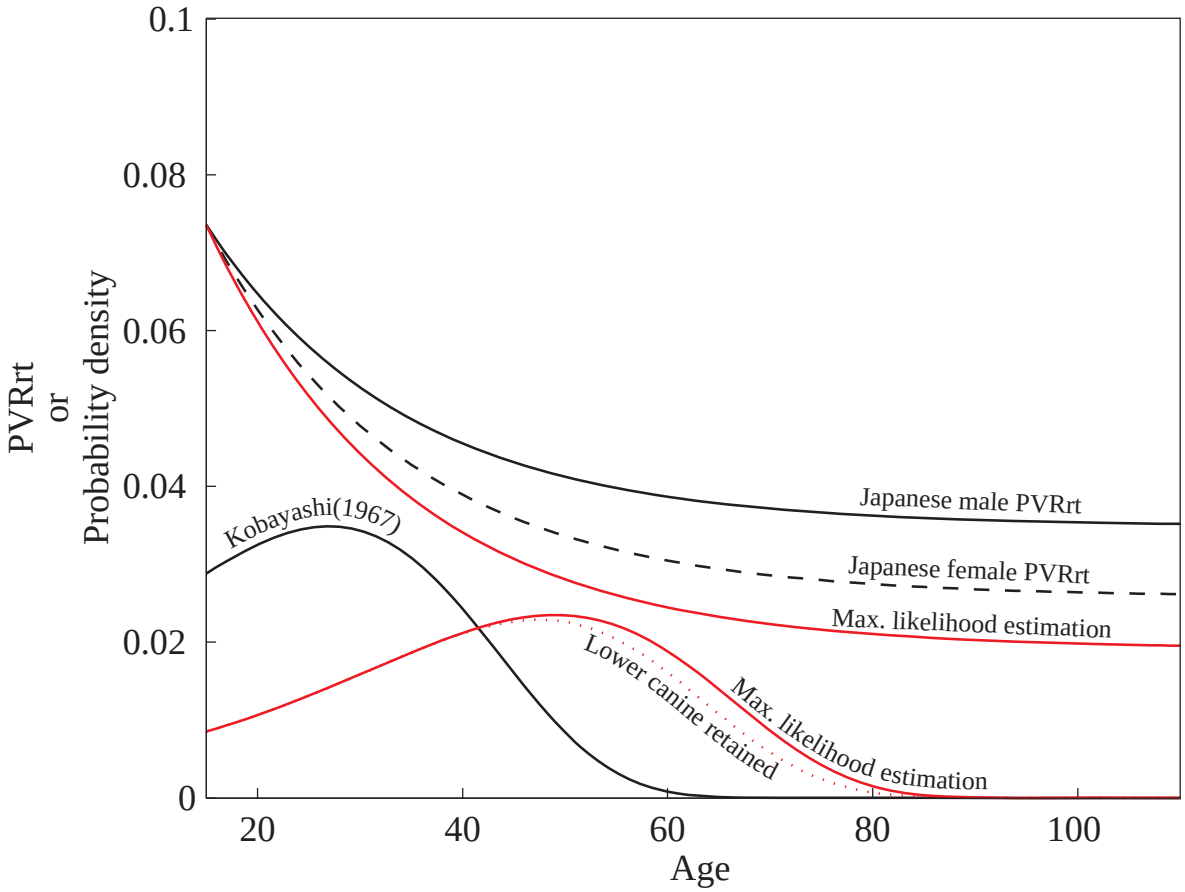

Figure 12. The age-at-death distribution and PVRrt reduction curve estimated by the maximum likelihood approach (red lines). Black lines are for comparisons. The vertical scale is coincidentally same for PVRrt and probability density of the age-at-death distribution. Red dotted line indicates the age distribution when those people missing the lower canines are excluded according to the tooth-loss model described in the text.

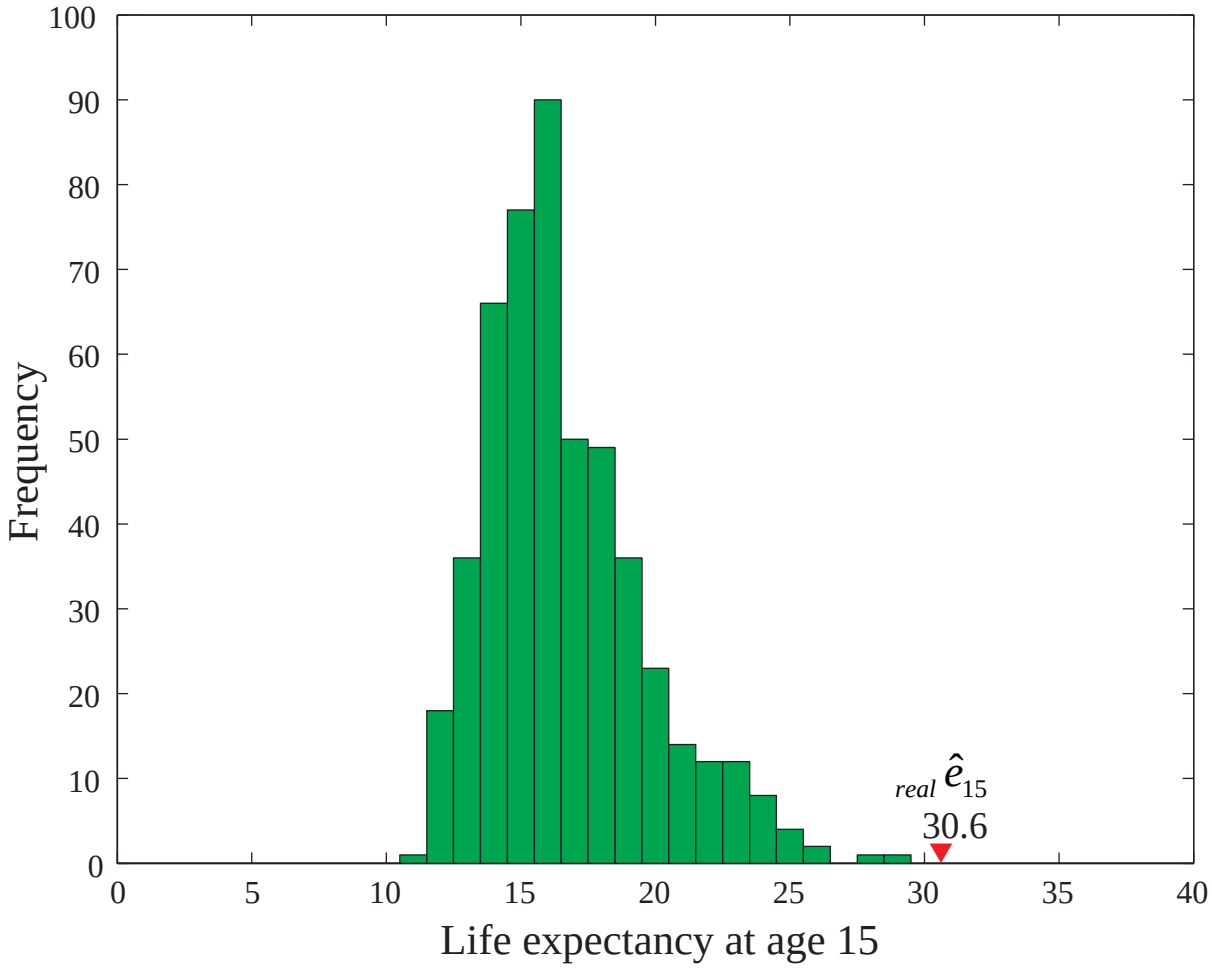

Figure 13. Comparison of the estimate from real samples and the distribution of the estimate from pseudo-samples generated upon the null hypothesis. $_{real}\hat{e}_{15}$ is the life expectancy at age 15 estimated by the maximum likelihood approach from the real Jomon samples. Green bars show the distribution of the estimations from computer-generated samples based upon the null hypothesis that the age-at-death distribution estimated by Kobayashi (1967) is true (n=500).

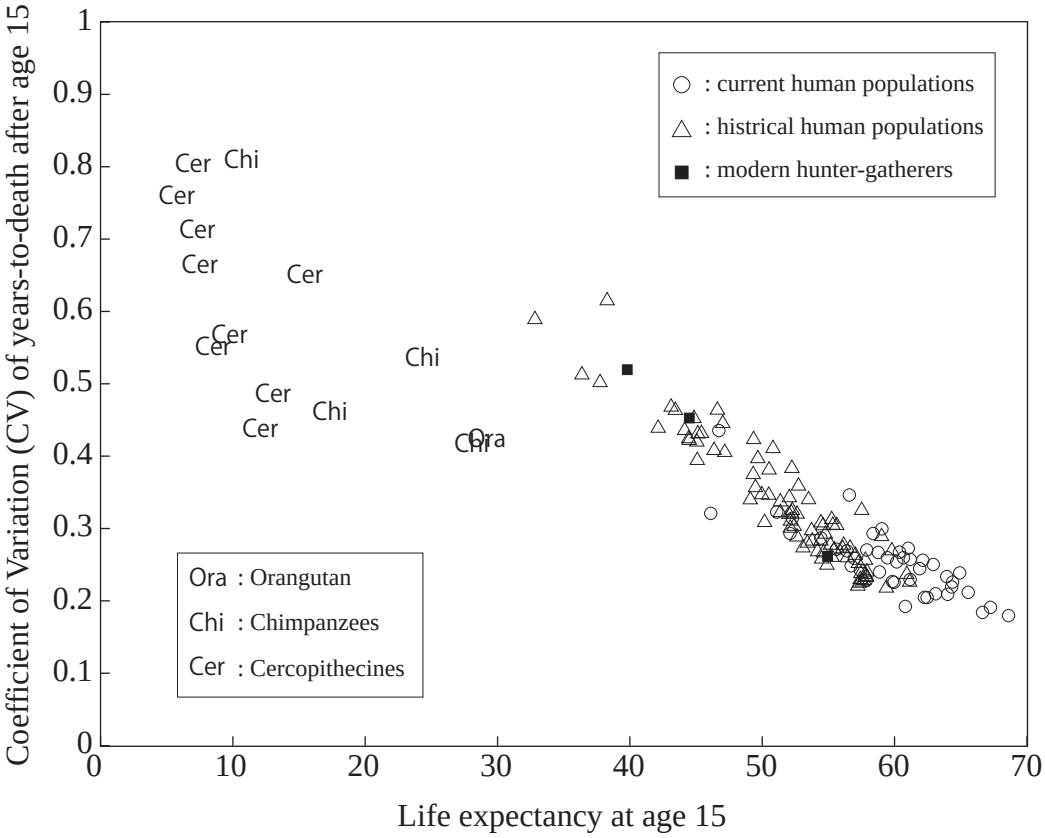

Figure 14. The scatter diagram of life expectancy at 15 and coefficient of variation (CV) of years-to-death after age 15. Those values were obtained by fitting the Gompertz model to the reported mortality data. See appendix A for the methods to fit the model. See Table 5 for the sources of the data.

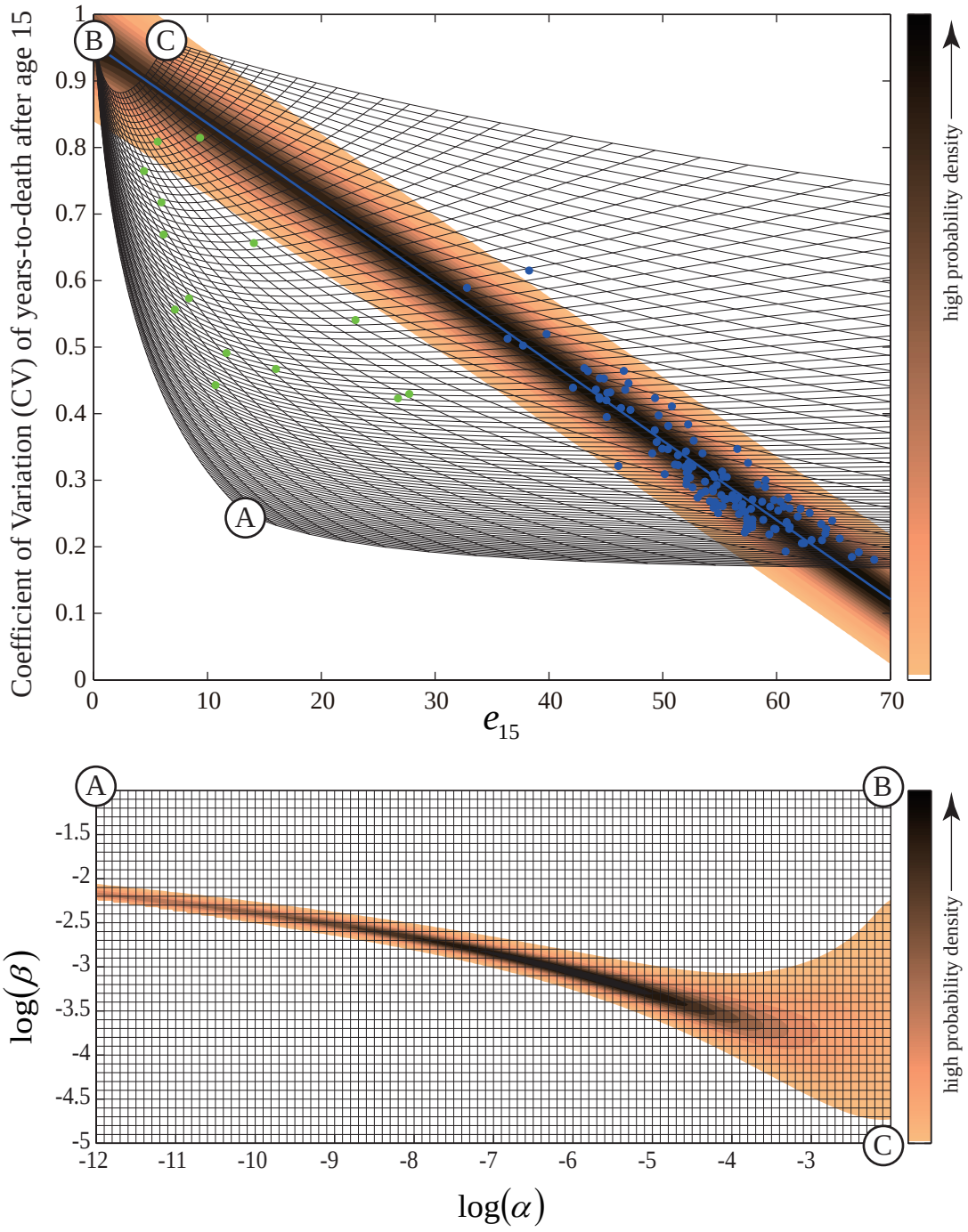

Figure 15. The non-uniform prior probability density distributions in the scale of e_{15}–CV (upper) and the scale of log(α)–log(β) (lower). In the upper picture, the blue dots indicate the human populations, while green dots indicate the non-human populations. The blue line in the upper picture is the regression line based on the human populations. The density was set to distribute along this line. The copper color indicates the probability density. The mesh in the lower picture corresponds to that in the upper picture showing the transformation between the scales.

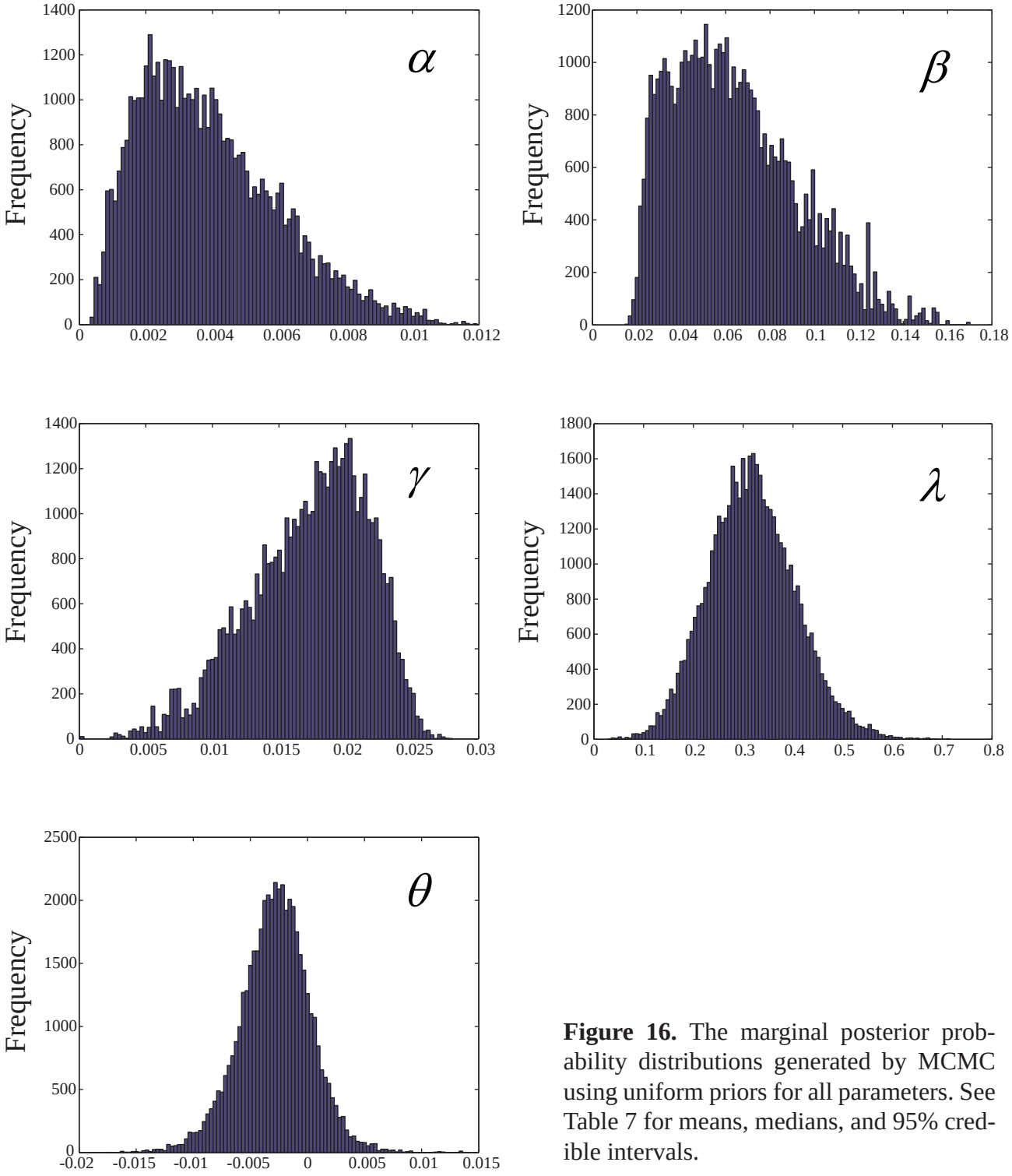

Figure 16. The marginal posterior probability distributions generated by MCMC using uniform priors for all parameters. See Table 7 for means, medians, and 95% credible intervals.

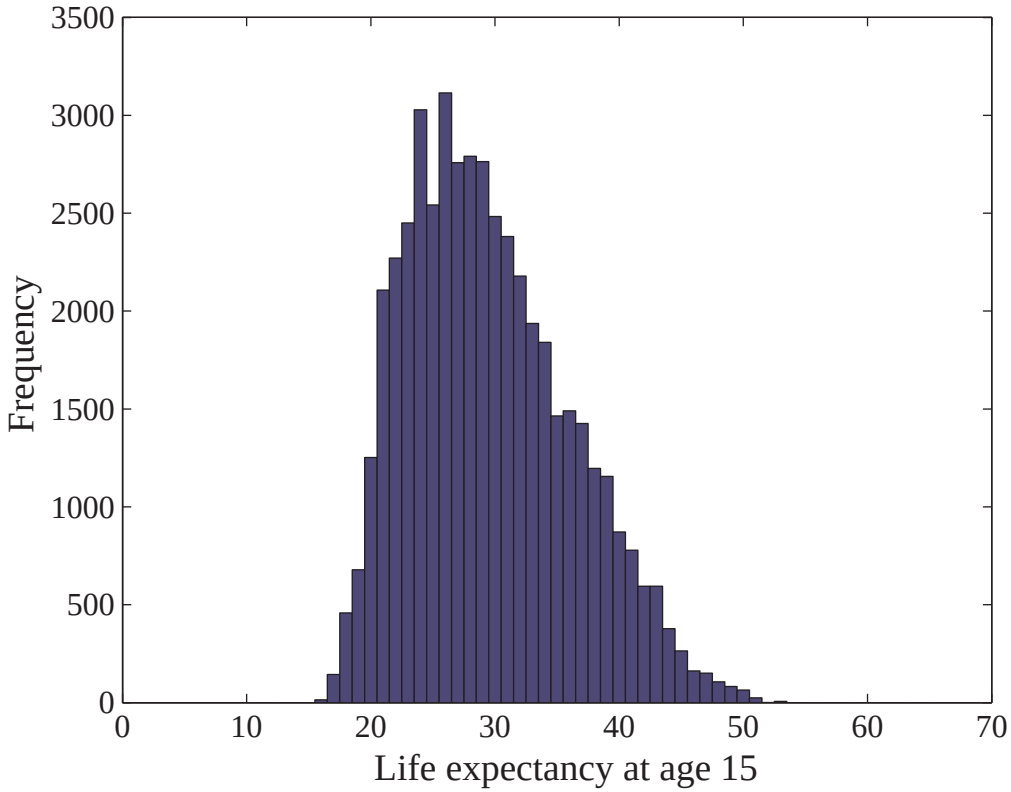

Figure 17. The posterior probability distribution of life expectancy for Jomon people at age 15, generated by MCMC using uniform priors for all parameters. See Table 7 for the mean, median, and 95% credible interval.

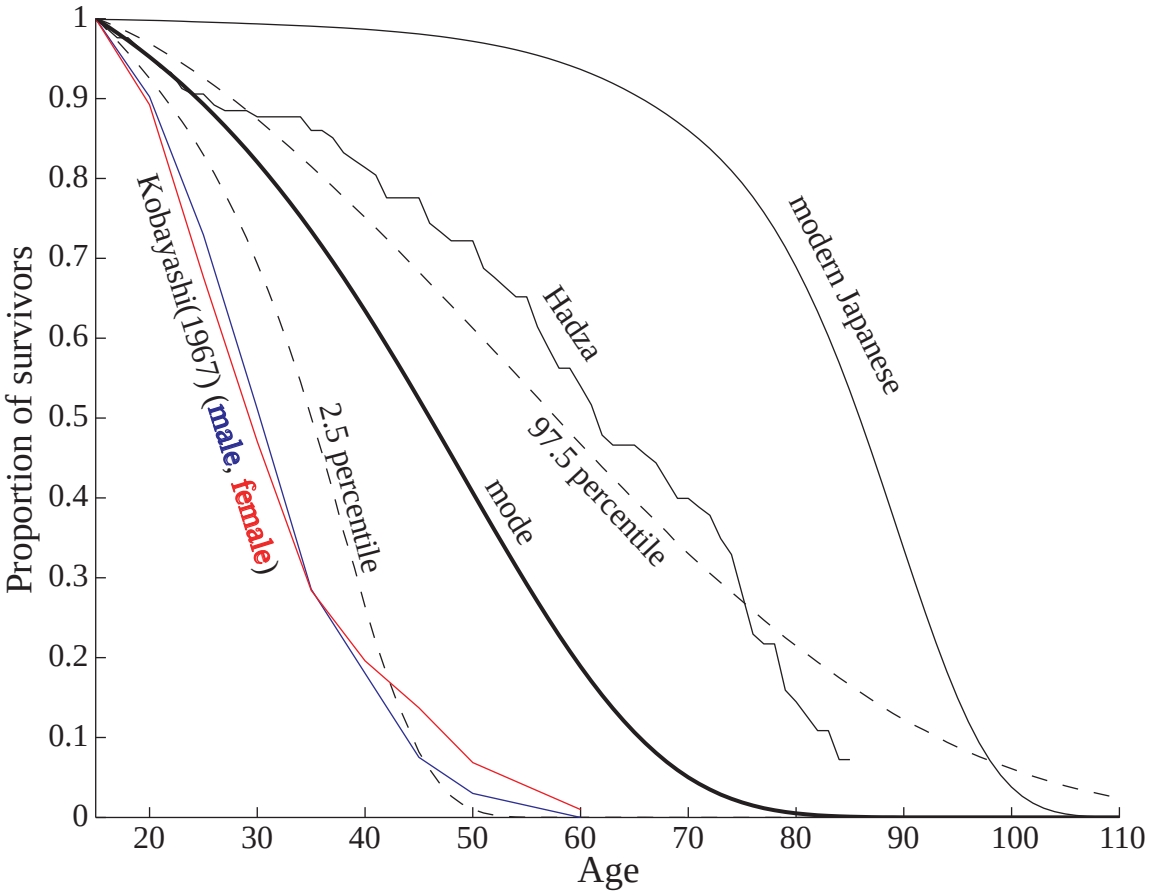

Figure 18. The survival curve drawn by the mode values of the posterior distribution when uniform priors were used for all parameters (bold solid line). The interval between 2.5 percentile and 97.5 percentile lines (dashed lines) indicates the interval below/above which 2.5 percent of survival curves generated by MCMC pass (i.e., 95% credible interval).

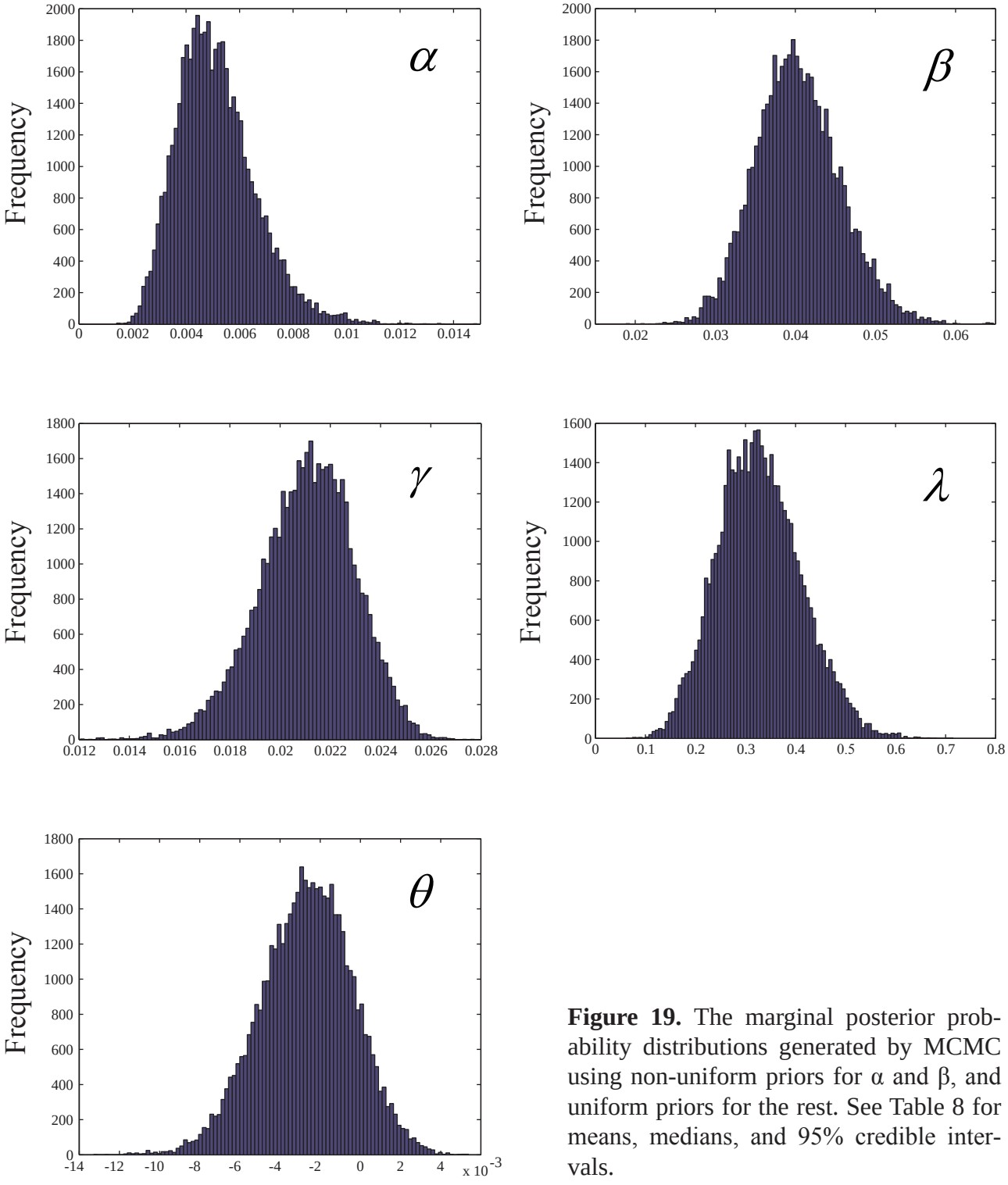

Figure 19. The marginal posterior probability distributions generated by MCMC using non-uniform priors for α and β, and uniform priors for the rest. See Table 8 for means, medians, and 95% credible intervals.

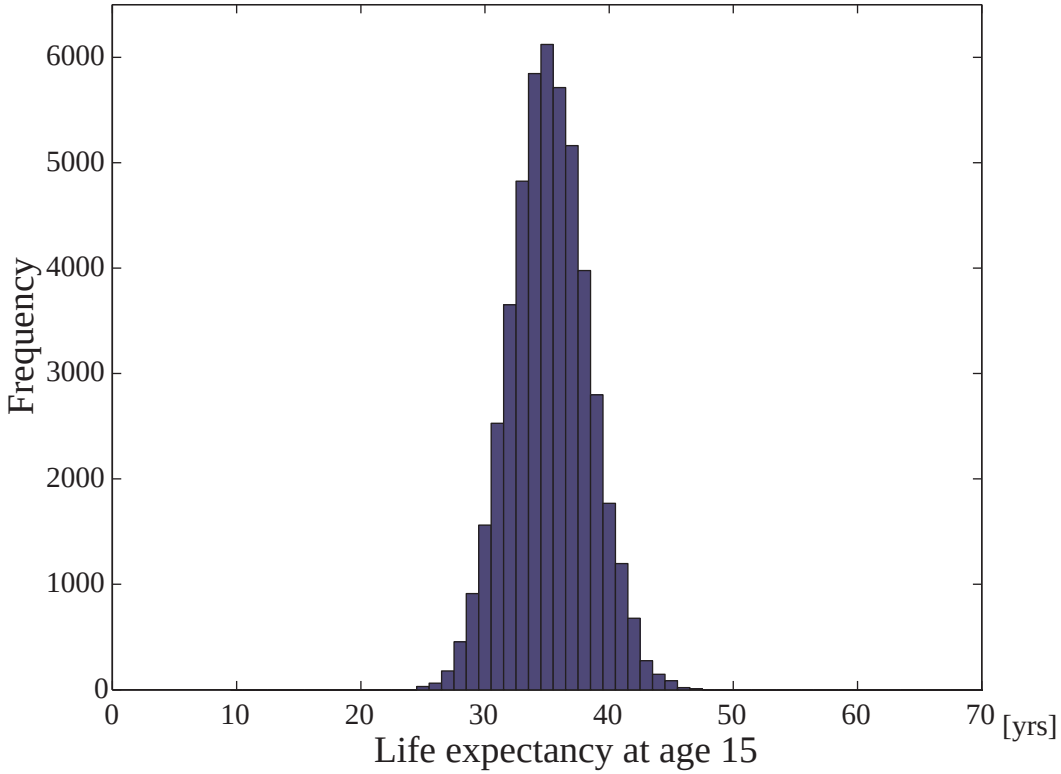

Figure 20. The posterior probability distribution of life expectancy for Jomon people at age 15, generated by MCMC using non-uniform priors for α and β, and uniform priors for the rest. See Table 8 for the mean, median, and 95% credible interval.

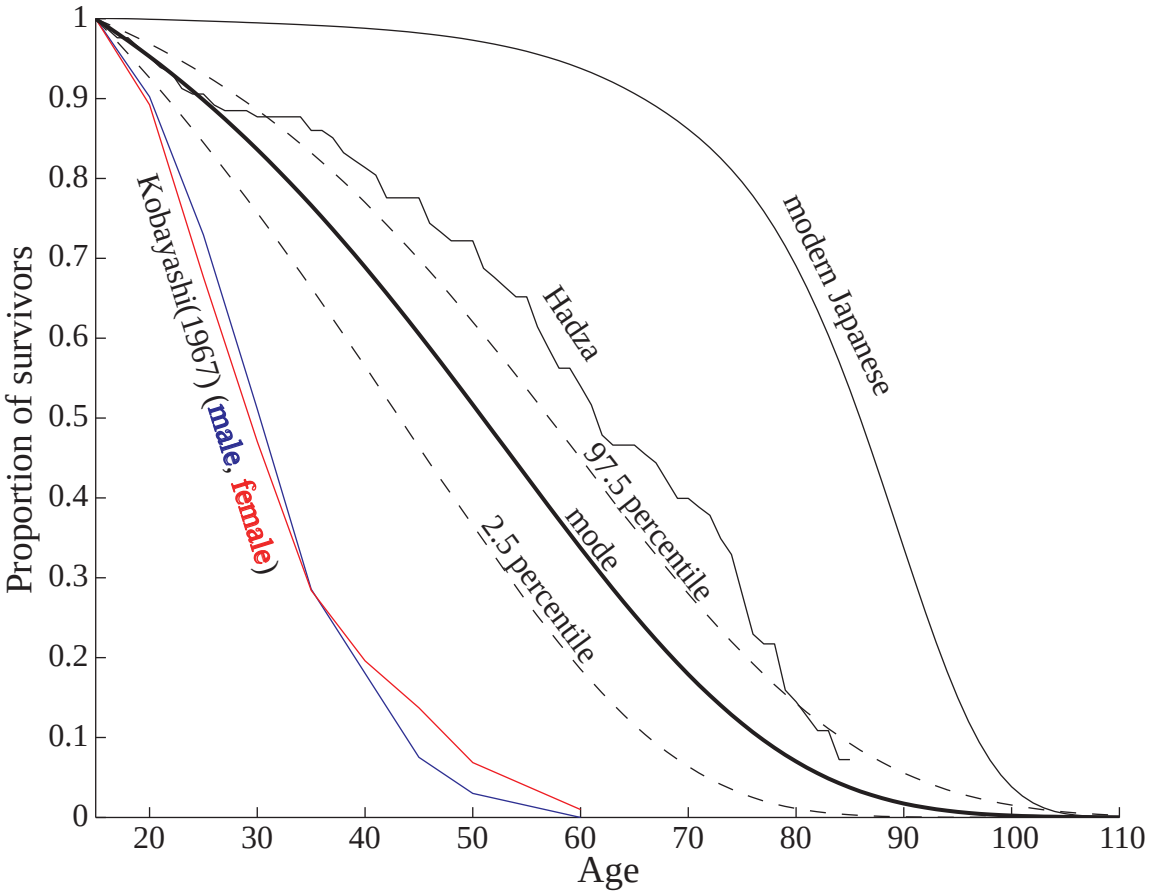

Figure 21. The survival curve drawn by the mode values of the posterior distribution when non-uniform prior was used for α and β, and uniform priors were used for the rest (bold solid line). The interval between 2.5 percentile and 97.5 percentile lines (dashed lines) indicates the interval below/above which 2.5 percent of survival curves generated by MCMC pass (i.e., 95% credible interval).

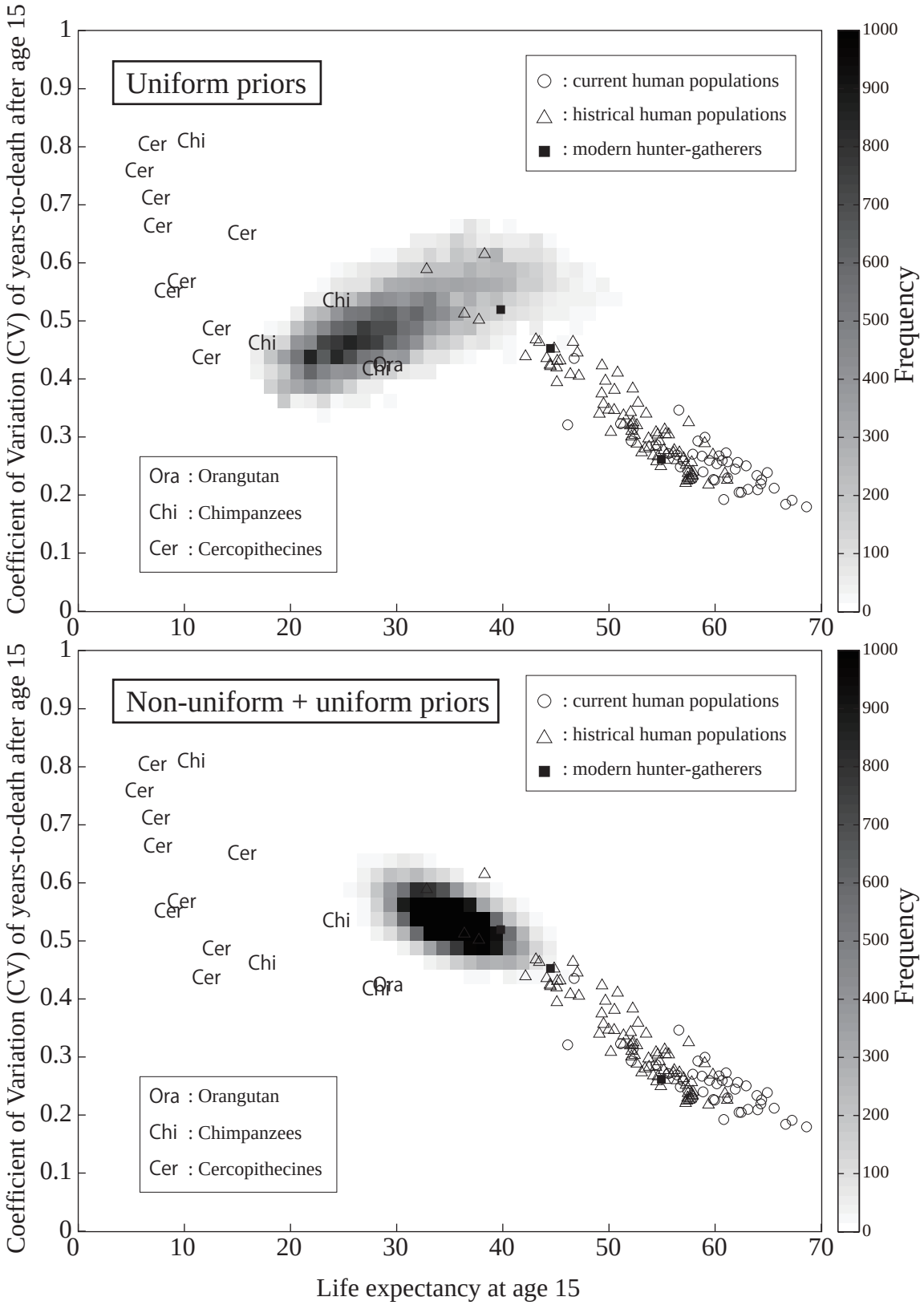

Figure 22. The comparison of the results from the two prior assumptions. The gray scale indicates the posterior probability density represented by the frequency of samples generated by MCMC (n=48,000). Those distributions were superimposed on Figure 14. It can be comfirmed that the non-uniform prior probability properly precluded the unlikely survival patterns as human.

Appendices

Appendix A

To fit the Gompertz model to the reported demographic data, the least square method or maximum likelihood method was used. The type of the demographic data collected for this study could be classified in to the following three types:

(1) Data where the age-specific probability of death (i.e., ${}_{\Delta x}q_x$, where x is starting age and Δx is span of the age-class) or the age-specific mortality rate (i.e., ${}_{\Delta x}m_x$, the same description as for ${}_{\Delta x}q_x$) was the most foundational information.

(2) Data where the numbers of survivors and deaths in each age-class during the observation period were available.

(3) Data where the number of death in each age-class during the observation period was available.

The case (1) was the most frequent case. In this case, the survival rate (l_x) was calculated from ${}_{\Delta x}q_x$ or ${}_{\Delta x}m_x$ for each sex, if sexes were separated. Then, the sexes were combined assuming male–female ratio of 105:100 at birth. If data at birth were not available, the ratio of 1:1 was assumed at the youngest age available. Then, the Gompertz survival curve $s_{15}(x)$ was fitted to the standardized survival profile (l_x / l_{15}) by the least square method. The resulting Gompertz parameters α and β were regarded as those for the population.

In the case (2), the likelihood function $l(\alpha,\beta)$ was calculated as

$$l(\alpha,\beta)=\prod_{i=1}^{N}\left(1-\frac{s_{15}(x_i)-s_{15}(x_i+\Delta x_i)}{s_{15}(x_i)}\right)^{n_{si}}\cdot\left(\frac{s_{15}(x_i)-s_{15}(x_i+\Delta x_i)}{s_{15}(x_i)}\right)^{n_{di}}, \qquad \text{(A1)}$$

where, N denotes the number of age-classes, and x_i, Δx_i, n_{si}, and n_{di} denote the starting age, the span, the number of survivors, and the number of death of the age-class i. The sexes were combined for the numbers of survivors and death. The (α,β) was determined so as to maximize the $l(\alpha,\beta)$.

In the case (3), the population was assumed to be stationary (i.e., no population growth nor decline and no secular change in the mortality and fertility profiles). And, the likelihood function $l(\alpha,\beta)$ was

calculated as

$$l(\alpha,\beta)=\prod_{i=1}^{N}\left(\frac{s_{15}(x_i)-s_{15}(x_i+\Delta x_i)}{s_{15}(x_1)}\right)^{n_{di}} . \qquad \text{(A2)}$$

The sexes were combined for the number of death. The (α,β) was determined so as to maximize the $l(\alpha,\beta)$.

For all the cases above, the reported data < 15 years of age were discarded when fitting the model except for cercopithecine monkeys. For cercopithecine monkeys, the data ≥ 5 years of age (assumed age of the maturity) were used to fit the Gompertz model, due to the scantiness of the data ≥ 15. Furthermore, for cercopithecine monkeys, only female data were used, since male data were occasionally unavailable.

Appendix B

The data of the dental survey by Ministry of Health, Labour and Welfare (undated) consisted of the number of people who had right lower canine and the number of people who don't, for each of 5-year age-classes. The numbers were divided by 10 and rounded down to the nearest integer just for computational efficiency. The data for the sexes were combined. The age of each person was assumed to be the mid point of the age class. The likelihood function $l(T_M,T_S)$ for the log-probit model was

$$l(T_M,T_S)=$$
$$\prod_{i=1}^{N}\left\{\int_0^{x_i}\frac{1}{t\sqrt{2\pi}\cdot T_S}\exp\left[-\frac{1}{2}\left(\frac{\log(t)-T_M}{T_S}\right)^2\right]\cdot dt\right\}^{n_{mi}}\cdot\left\{1-\int_0^{x_i}\frac{1}{t\sqrt{2\pi}\cdot T_S}\exp\left[-\frac{1}{2}\left(\frac{\log(t)-T_M}{T_S}\right)^2\right]\cdot dt\right\}^{n_{ri}}, \qquad \text{(B1)}$$

where N denotes the number of age-classes, and x_i, n_{mi}, and n_{ri} denote the mid point, the number of people who miss the right lower canine, and the number of people who retain it, respectively, in the age-class i. T_M and T_S were determined by maximizing this likelihood function.